

1 **Title: A structural dendrogram of the actinobacteriophage major capsid proteins**
2 **provides important structural insights into the evolution of capsid stability**

3
4 **Authors:** Jennifer M. Podgorski¹, Krista Freeman², Sophia Gosselin¹, Alexis Huet³,
5 James F. Conway³, Mary Bird¹, John Grecco¹, Shreya Patel¹, Deborah Jacobs-Sera²,
6 Graham Hatfull², Johann Peter Gogarten^{1,4}, Janne Ravantti⁵, Simon White^{1*}

7
8 **Affiliations**

9
10 **1.** Biology/Physics Building, Department of Molecular and Cell Biology, University of Connecticut, 91
11 North Eagleville Road, Unit-3125. Storrs, CT 06269-3125, USA

12
13 **2.** Clapp Hall, Department of Biological Sciences, University of Pittsburgh, 4249 Fifth Avenue, Pittsburgh,
14 PA 15260, USA

15 **3.** Department of Structural Biology, University of Pittsburgh School of Medicine, Pittsburgh, PA, USA.

16 **4.** Institute for Systems Genomics, University of Connecticut, Storrs, CT 06268-3125, USA.

17 **5.** University of Helsinki, Molecular and Integrative Biosciences Research Programme, Helsinki, Finland.

18
19 * Author to whom correspondence should be addressed.

20

21

22

23

24

25 **Abstract**

26

27 Many double-stranded DNA viruses, including tailed bacteriophages (phages) and
28 herpesviruses, use the HK97-fold in their major capsid protein to make the capsomers
29 of the icosahedral viral capsid. Following the genome packaging at near-crystalline
30 densities, the capsid is subjected to a major expansion and stabilization step that allows
31 it to withstand environmental stresses and internal high pressure. Several different
32 mechanisms for stabilizing the capsid have been structurally characterized, but how
33 these mechanisms have evolved is still not understood. Using cryo-EM structure
34 determination, structural comparisons, phylogenetic analyses, and Alphafold
35 predictions, we have constructed a detailed structural dendrogram describing the
36 evolution of capsid structural stability within the actinobacteriophages. The cryo-EM
37 reconstructions of ten capsids solved to resolutions between 2.2 and 4 Ångstroms
38 revealed that eight of them exhibit major capsid proteins that are linked by a covalent
39 cross-linking (isopeptide bond) between subunits that was first described in the HK97
40 phage. Those covalent interactions ultimately lead to the formation of mutually
41 interlinked capsomers that has been compared to the structure of chain mail. However,
42 three of the closely related phages do not exhibit such an isopeptide bond as
43 demonstrated by both our cryo-EM maps and the lack of the required residue. This work
44 raises questions about the importance of previously described capsid stabilization
45 mechanisms.

46 **Introduction**

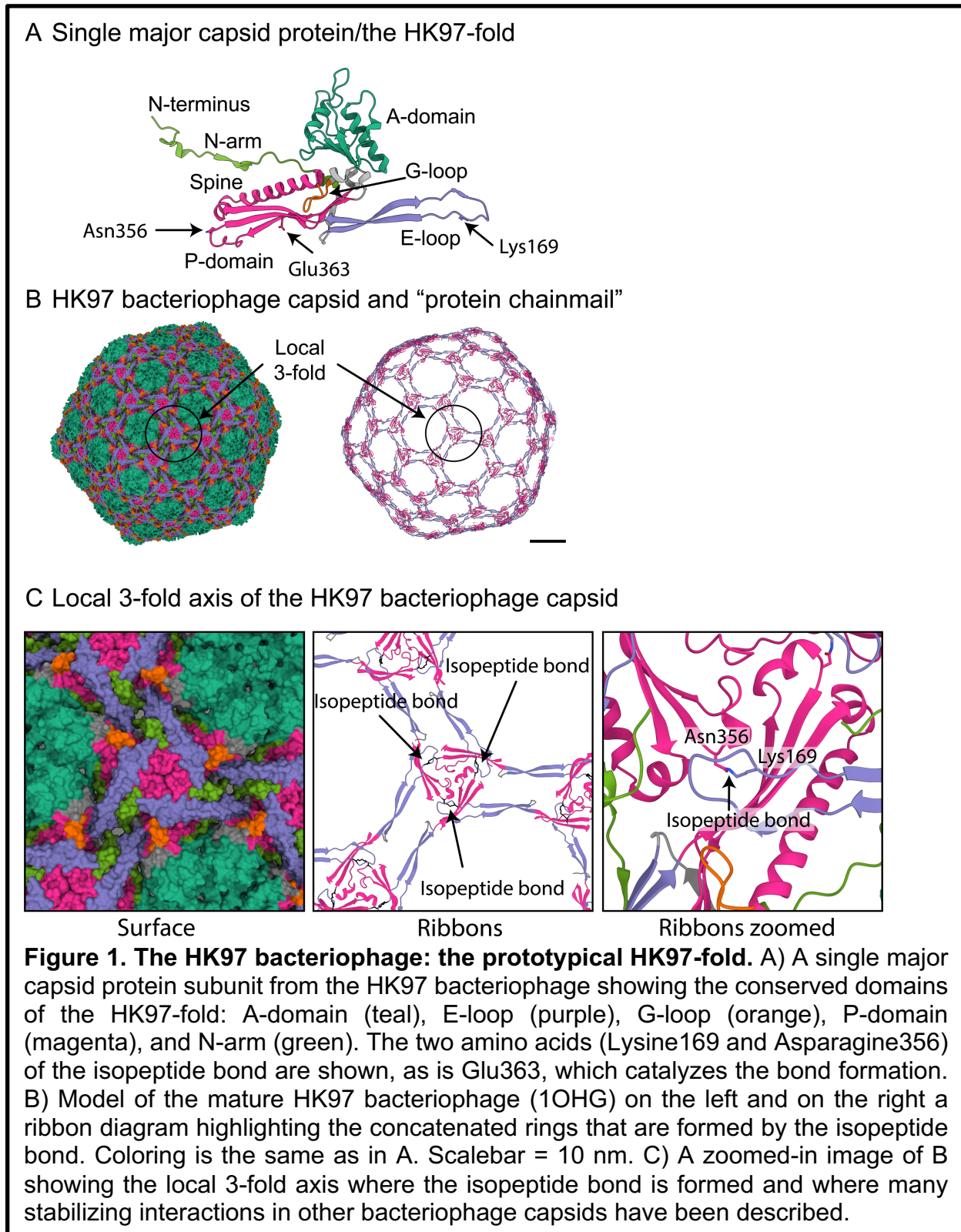
47

48 The HK97-fold (Figure 1 A) is ubiquitous in the biosphere and has been identified in
49 viruses that infect the three domains of life^{1,2,3}, as well as encapsulins⁴: protein shells
50 used by bacteria for gene transfer and reaction confinement⁵. It is found across the
51 Caudovirales order (the double-stranded DNA tailed phages), which is one of the
52 largest groups of viruses in the biosphere and plays major roles in bacterial evolution
53 and in carbon/nitrogen/phosphorus cycling⁶. Actinobacteriophages (bacteriophages
54 infecting actinobacterial hosts) have been intensively studied with over 20,000 individual
55 isolates, the vast majority of which are dsDNA phages. These phages are the central
56 focus of integrated research-education programs^{7,8}, have provided tools for
57 *Mycobacterium* genetics⁹, and show promise as therapies for drug-resistant
58 *Mycobacterium* infections^{10,11}.

59

60 Most of the major capsid proteins in the tailed phages use the HK97-fold (Figure 1 A) as
61 the foundational block to build the capsid (Figure 1 B). To date, all structurally
62 characterized HK97-folds have several conserved domains^{12,13}. They include the A
63 domain (Figure 1A, teal) that forms the central core of the hexamer and pentamer
64 capsomers of the capsid; the P-domain (Figure 1A, magenta) where the long spine helix
65 is located; as well as the E-loop (Figure 1A, purple) and N-arm (Figure 1A, green). The
66 E-loop and N-arm make long-range contacts with other major capsid proteins and play
67 important roles in capsid stability¹⁴. The viral major capsid protein that uses the HK97-

68 fold is assembled into an icosahedral shell consisting of eleven pentamers and different
69 numbers of hexamers of the major capsid protein depending on the size and shape of



70 the capsid. The icosahedral capsid is described by a T number that defines the number
71 of major capsid proteins in the icosahedral shell - equal to the T number multiplied by
72 sixty¹⁵. Within the dsDNA tailed phages, one pentamer is replaced by the portal to which
73 the tail is bound and through which the DNA is packaged and then released.

74

75 The stability of the mature capsid is a key factor in the evolutionary success of
76 phages¹⁶. The capsid needs to withstand various environmental conditions, and the
77 pressure of the packed DNA genome^{17,18,19}. The local 3-fold axes for each capsomer,
78 where the P-domains of the pentamer and hexamer capsomers intersect, are thought to
79 be important for capsid stability¹⁶ (Figure 1 B and C highlights one such 3-fold axis in
80 the HK97-fold). The tailed phages use several different mechanisms to stabilize the
81 capsid local 3-fold axes. The most common is a minor capsid protein, or 'cement', that
82 binds to the local 3-fold axis and makes several contacts with the surrounding major
83 capsid subunits^{20,21}. Others use catenated rings, with either non-covalent²² or covalent
84 bonding²³ mechanisms, that connect the major capsid proteins around the local 3-fold
85 axis¹⁴. The major capsid protein of the HK97 phage (in which the HK97-fold was first
86 characterized) uses a covalent isopeptide bond to cross-link a conserved asparagine
87 (Asn356) in the P-domain of one major capsid protein with a conserved lysine (Lys169)
88 in an adjacent E-loop of a different major capsid protein²³ (Figure 1 B and C). The
89 cross-linking is catalyzed by a nearby glutamic acid (Glu363) on a third major capsid
90 protein subunit and aided by three other amino acids that form a hydrophobic pocket²⁴.
91 The cross-linking of all the major capsid proteins results in the catenated rings or
92 "protein chainmail" that stabilizes the capsid around the local 3-fold axes (Figure 1 C).

93 Some phages have been characterized, for example, T5²⁵, T7²⁶, and phiRSA1²⁷, that
94 rely solely on intracapsomeric interactions and do not use cement or non-
95 covalent/covalent bonding mechanisms. These different mechanisms of capsid
96 stabilization make the HK97-fold highly adaptable and able to survive a wide variety of
97 environments, from soil to hot springs and allows for the formation of structurally very
98 diverse capsids that range in size from relatively small 50 nm diameter capsids^{28,29,30} to
99 hundreds of nanometers in diameter “giant” capsids^{31,32}.

100

101 High-resolution structures of over twenty-five tailed phage capsids²¹⁻⁵⁰, viruses that
102 infect archaea², and the human pathogenic Herpesvirus³ show that the HK97-fold is well
103 conserved, even among viral capsids sharing little or no amino acid sequence similarity
104 and using several different capsid stability mechanisms. However, these structures are
105 from viruses that infect diverse hosts across all three domains of life and are so
106 divergent from one another that only limited conclusions can be made about their
107 evolution. We, therefore, carried out a systematic investigation of closely related phages
108 infecting actinobacterial hosts to understand how capsid stability mechanisms are
109 conserved and how they have evolved.

110

111

112

113

114

115

116 **Materials and Methods**

117 ***Production and purification of Phages for Cryo-Electron Microscopy***

118 Phages were produced as previously described⁵¹. Briefly, twenty webbed plates were
119 made for each phage with their host (Supporting Information Table 1) in top agar on
120 Luria agar plates and incubated overnight at the temperatures shown in Supporting
121 Information Table 1. Phages were extracted from the webbed plates using 5 mL of
122 Phage Buffer (10 mM Tris-HCl pH 7.5, 10 mM MgSO₄, 68 mM NaCl, 1 mM CaCl₂) and
123 incubated overnight at room temperature to allow diffusion of the phages into the Phage
124 Buffer. The lysate was aspirated from the plates and centrifuged at 12,000× *g* for 15 min
125 at 4 °C to remove cell debris. Phage particles were then pelleted using an SW41Ti
126 swinging bucket rotor (Beckman Coulter, Brea, CA) at 30,000 rpm for 3 hours using
127 12.5 mL open-top poly clear tubes (Seton Scientific, Petaluma, CA). The phage
128 particles in the pellet were then resuspended in 7 mL of Phage Buffer by gentle rocking
129 overnight at 4 °C. The new phage lysate was subjected to isopycnic centrifugation with
130 the addition of 5.25 g of CsCl to the 7 mL of phage lysate. The CsCl/phage solutions
131 were centrifuged at 40,000 rpm in an S50-ST swinging bucket rotor (Thermofisher
132 Scientific, Waltham, MA) for 16 h and the phage particle band (that appeared roughly
133 halfway down the tube) was removed via side puncture with a syringe and needle.
134 Phage particles were then dialyzed three times against Phage Buffer to remove CsCl.
135 To do this the ~1 mL of purified phages was placed into a Tube-O-Dialyzer Micro (G-
136 Biosciences, St Louis, MO) with a 50 kDa molecular weight cut-off. The phages were
137 then concentrated a final time by pelleting them at 75000 rpm in an S120-AT2 fixed

138 angle rotor (Beckman Coulter, Brea, CA). The phage particles were then resuspended
139 in 20 μ L of Phage Buffer with gentle pipetting.

140

141 ***Preparation of Cryo-Electron Microscopy Grids***

142 Five microliters of concentrated phage particles (approximately 10 mg/mL) were added
143 to Au-flat 2/2 (2 μ m hole, 2 μ m space) cryo-electron microscopy grid (Protochips,
144 Morrisville, NC, USA) using a Vitrobot Mk IV (Thermo Fisher Scientific, Waltham,
145 Massachusetts, USA). Grids were blotted for 5 s with a force of 5 (a setting on the
146 Vitrobot) before being plunged into liquid ethane. For Muddy phage, three microliters of
147 concentrated phage particles were added to a freshly glow-discharged Quantifoil R2/1
148 grid (Quantifoil Micro Tools GmbH, Großlöbicha, Germany) and plunge-frozen with a
149 Vitrobot Mk IV into a 50:50 mixture of liquid ethane:propane⁵²

150

151 ***Cryo-Electron Microscopy***

152 Data were collected on a 300 keV Titan Krios (Thermo Fisher Scientific, Waltham,
153 Massachusetts, USA) at the Pacific Northwest Center for Cryo-EM with either a K3 or
154 Falcon 3 direct electron detector (Gatan, Pleasanton, CA, USA). The data for Muddy
155 was collected on a 300 keV Titan Krios 3Gi at the University of Pittsburgh with a Falcon
156 3 direct electron detector (Thermo Fisher Scientific, Waltham, Massachusetts, USA).
157 Supporting Table 2 provides the collection parameters for each phage.

158

159 ***Cryo-Electron Microscopy Data Analysis***

160 Relion 3.1.1⁵³ was used for phage capsid reconstructions using the standard workflow.
161 CTF Refinement was performed using the default settings. Bayesian polishing was not
162 performed since it made little improvement on resolution (approx. 0.1 Å for Bobi when
163 attempted) for the computational time. Ewald sphere correction was carried out for each
164 particle using the `relion_image_handler` command that is included with Relion. The
165 `mask_diameter` value used in the Ewald sphere correction is reported in Supporting
166 Table 2.

167

168 ***De novo model building***

169 The amino acid sequences of the major capsid proteins were folded with AlphaFold⁵⁴
170 version 2.0 using the default settings on a local workstation. The highest ranked
171 prediction model was fitted into the cryo-EM map using ChimeraX⁵⁵ version 1.3 and the
172 “Fit in Map” command. Coot⁵⁶ version 0.9.2 was then used to manually fit the model into
173 the density using the “Stepped sphere refine active chain” provided by the python script
174 developed by Oliver Clarke⁵⁷. Any remaining protein backbone that was incorrectly
175 placed was then manually moved into the correct density. All maps were of sufficient
176 quality for side chains to be easily recognizable. The real-space refinement tool of
177 Phenix⁵⁸ version 1.19.2-4158 was used with default settings to refine the model and
178 Coot was then used to manually fix the majority of the issues identified through Phenix.
179 The final step was to use the ChimeraX plugin, Isolde⁵⁹ version 1.3, to refine the major
180 capsid protein model. The whole model simulation was used with a temperature of 20
181 °K. All other parameters were default. After the first model was completed, the

182 asymmetric unit of the capsid was created using a similar workflow with a final Isolde
183 refinement of the entire asymmetric unit.

184

185 **Phylogenetic analysis of the major capsid protein amino acid sequences**

186 Amino acid sequences of the three major capsid protein phams (named as of July 2021:
187 4631, 15199, 57445) were downloaded from PhagesDB⁶⁰ and merged into a single
188 multifasta file. The divergent nature of these protein sequences required an alignment
189 algorithm that could permit a large number of gaps in our multiple sequence alignment.
190 To that end, we aligned the major capsid proteins using MAFFT (v7.453)⁶¹ with the
191 following parameters: globalpair, unalignlevel 0.8, leavegappyregion, and maxiterate
192 1000.

193

194 A maximum likelihood phylogeny was created from the multiple sequence alignment
195 using IQTree (v1.6.6)⁶² with the following parameters: ModelFinder Plus⁶³ (-m MFP),
196 and 100 non-parametric bootstraps (-bb 100). The model finder chose an LG model with
197 empirical frequencies and five rate categories (LG+F+R5) as the most likely model
198 based on the Bayesian information criterion. The resulting phylogeny was visualized in
199 Figtree (v1.4.4)⁶⁴. Nodes were collapsed only when the collapsed node contained a
200 single pham from a single phage subcluster.

201

202 **Alphafold of major capsid proteins**

203 To create the structural dendrogram, we used Alphafold to predict the three-dimensional
204 protein fold of a representative major capsid protein from each cluster (139 total

205 clusters), as well as every Singleton (62) major capsid protein. All protein sequences
206 were obtained from the actinobacteriophage database (PhagesDB)⁶⁰ and Phamerator⁶⁵
207 in July 2021. For the few clusters (A, BN, CZ, DN, and F) that have more than one
208 major capsid protein phamily, we folded a representative of each major capsid protein
209 phamily from that cluster. There are forty-two annotated major capsid protein phamilies
210 in the actinobacteriophages, spread across the 201 clusters and Singletons. In total, five
211 clusters (DK, DS, EK, EM, and FC) and eight Singletons have no annotated major
212 capsid protein and were therefore excluded from this analysis. The 18 total excluded
213 phages account for less than 0.5% of the total number of annotated
214 actinobacteriophages, so their exclusion is unlikely to skew the results. Cluster BO,
215 which contains two phages, was also excluded from this analysis since they do not use
216 the HK97-fold in their major capsid protein and are part of the Tectiviridae family of
217 viruses. In total, 201 major capsid proteins were predicted with the default Alphafold
218 settings and the major capsid protein amino acid sequence as input. The model with the
219 highest confidence was used in the structural map. PDB files were manually truncated
220 to remove the N-arm and the delta domain if present. The N-arm was truncated to
221 approximately where the N-arm crosses behind the spine helix of the major capsid
222 protein. The fasta files and PDB files of the predicted full-length and truncated major
223 capsid proteins can be found in Supporting Information.

224

225 **Creation of a structural dendrogram using Homologous Structure Finder**

226 In this study, we applied automatic structure alignment and the structure-based
227 classification method Homologous Structure Finder (HSF)⁶⁶, which allows

228 comprehensive comparisons of proteins, not only within a protein family (such as RNA-
229 dependent RNA polymerase)⁶⁷ but also between protein families and superfamilies,
230 significantly extending the depth of sequence-based phylogenies⁶⁶. HSF identifies the
231 equivalent residues for a pair of protein structures by comparing a set of amino acid
232 properties (e.g., physiochemical properties of amino acids, local geometry, backbone
233 direction, local alignment, and C α distances)⁶⁶. The two protein structures that are the
234 most similar based on the properties are merged into a common structural core which
235 then represents the pair in the later iterations. Next, the structure or a core from a
236 previous iteration, best matching to an existing core or to a single structure not in any
237 core yet, is merged either to a core or to another structure. The iterations are continued
238 until all the protein structures are part of a clustering and a single structural core is
239 identified for all the proteins in the data set. The equivalent residues in the structural
240 core can be considered homologous, similar to high-scoring columns of multiple
241 sequence alignment.

242
243 Pairwise comparison of the properties of the residues in the homologous positions of
244 the common structural core between the original structures results in a pairwise
245 distance matrix, which can be then used for constructing a structure-based distance
246 tree⁶⁶. The distances in such structure-based distance trees do not necessarily scale
247 with respect to time, as changes in protein structure may not be continuous. However,
248 the clustering of proteins in the structure-based distance tree constructed using HSF
249 has been shown to follow the sequence-based classification of proteins into protein
250 families, even when the common core contains less than 40 residues⁶⁷. Thus, structure-

251 based analysis is appropriate for a rough estimation of evolutionary events and
252 relationships between protein families when the proteins share little or no detectable
253 sequence similarity, and the accuracy of estimation of the evolutionary events increases
254 as the sequence similarity increases.

255

256 **Data Deposition**

257 PDB/EMDB/EMPIAR (unprocessed micrographs) accession numbers are as follows:

258

259 Adephagia: 8EC2/EMD-28012/EMPIAR-11200

260 Bobi: 8EC8/EMD-28015/EMPIAR-11201

261 Bridgette: 8ECI/EMD-28016/EMPIAR-11209

262 Cain: 8ECJ/EMD-28017/EMPIAR-11205

263 Che8: 8E16/EMD-27824/EMPIAR-11190

264 Cozz: 8ECK/EMD-28018/EMPIAR-11206

265 Muddy: 8EDU/EMD-28039/Not deposited in EMPIAR

266 Ogopogo: 8ECN/EMD-28020/EMPIAR-11207

267 Oxtober96: 8ECO/EMD-28021/EMPIAR-11208

268 Ziko: 8EB4/EMD-27992/EMPIAR-11195

269 **Results**

270

271 ***The actinobacteriophages have forty-two major capsid protein phamilies***

272 There are currently (August 2022) over 4000 sequenced and annotated
273 actinobacteriophages, which can be grouped into over 139 clusters and sub-clusters.
274 Clustering is based on shared gene content between phage genomes, such that a
275 phage is included in a cluster if it shares at least 35% of its genes with any member of
276 that cluster (e.g. Cluster A, Cluster B, etc). Therefore, phages within a cluster are
277 generally more globally similar to one another than to phages in other clusters. Some
278 clusters can be similarly divided into sub-clusters (e.g. Subcluster A1, Subcluster A2,
279 etc). Clusters range from having just two members (e.g. Cluster X) to over seven
280 hundred (Cluster A), with most having fewer than fifty. Additionally, there are sixty-six
281 “Singletons” (August 2022), those phages that have a genome that does not fit into an
282 existing cluster. These cluster/subcluster singleton groupings do not reflect firm
283 biological distinctions, as phage genomes are pervasively architecturally mosaic, and
284 phage populations likely span a continuum of diversity⁶⁸.

285

286 The shared gene content comparison used for clustering is done at the protein level
287 after genes have been translated and their products sorted into protein “phamilies”
288 using Phamerator⁶⁵ and a pipeline built on MMseqs2 (Gauthier and Hatfull, manuscript
289 in preparation)⁶⁹. A phamily⁶⁵ is defined as a group of related proteins and although built
290 with k-mer-based methods, proteins within a phamily typically have a minimum pairwise
291 20% amino acid identity. Amino acid sequence analysis of approx. 3200 major capsid

292 proteins shows that there are forty-two major capsid protein families (termed
293 phamilies/phams) within the actinobacteriophages database (July 2021). The majority of
294 the 139 phage clusters have a single major capsid protein phamily and, as shown in this
295 paper, it is possible to recapitulate most of the shared gene content-based phage
296 clustering using only the major capsid protein.

297

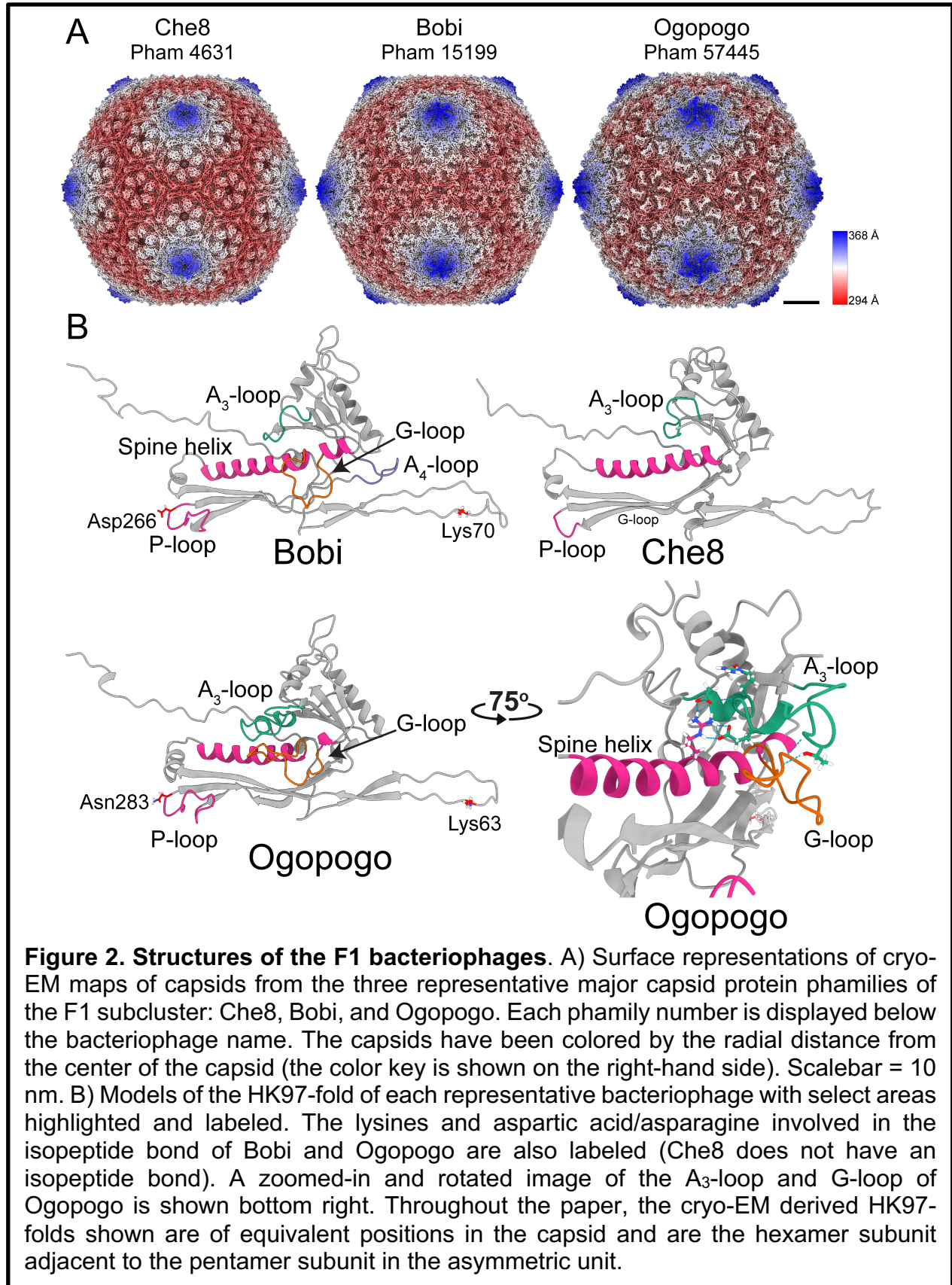
298 ***The F1 sub-cluster contains three major capsid protein phamilies***

299 Because of the mosaic nature of phage genomes, some cluster/subcluster groups (e.g.
300 A, BC, CZ, DN, and F) include multiple major capsid protein phamilies; Subcluster F1
301 has the most with three different major capsid protein phamilies. Previous structural
302 studies with the *Escherichia coli* CUS-3 and *Salmonella* P22 phages have shown that
303 major capsid proteins with minimal amino acid sequence identity (less than 15%) can
304 result in almost identical capsid morphologies and HK97-folds^{39,46}. We, therefore,
305 started the systematic investigation of the actinobacteriophages with the F1 major
306 capsid proteins to address whether the three major capsid protein phamilies in the F1
307 subcluster are the same HK97-fold with highly diverged amino acid sequences, or
308 whether they are three distinct folds.

309

310 In total, 180 phages within the F1 subcluster use one of three major capsid protein
311 phamilies; the three major capsid protein phamilies show a minimum of 97% amino acid
312 sequence identity within a phamily and a maximum of 15% between the phamilies.
313 Since the amino acid sequence identity is so high within each phamily, we chose a
314 representative phage from each of the major capsid protein phamilies. These

315 representatives are Che8 (phamily/pham number 4611, major capsid protein, gene
316 number = 6), Bobi (phamily 15199, major capsid protein, gene number = 7), and
317 Ogotogo (phamily 57445, major capsid protein, gene number = 8) for structural
318 analysis. Note: phamily numbers are subject to change but are accurate at the time of
319 writing (August 2022). Cryo-electron microscopy was used to determine a sub 3 Å map
320 (Figure 2 A) for each of the three representative phages (see Supporting Table 2 for
321 collection parameters, analysis, and final resolutions). The capsids all use the T=9
322 icosahedral architecture, with 540 copies of the major capsid protein, and are of similar
323 size (740 Å diameter) and internal volumes (approx. 3×10^7 Å³), which is expected since
324 they package double-stranded DNA genomes of very similar length (Supporting Table
325 1). The high-resolution data obtained from our studies allowed for *de novo* model
326 building of the major capsid protein's amino acid sequence into the corresponding map.
327 The resulting models of the three phages confirmed that each phage adopts the HK97-
328 fold in their major capsid protein (Figure 2 B).



330 A comparison of the three major capsid proteins, which have ~15% amino acid
331 sequence identity, revealed that the HK97-folds of the representative phages are very
332 similar to one another (Figure 2), with Root Mean-Square Deviation (RMSD) of atomic
333 position values <1.35 Å. While each fold is structurally similar to the original HK97-fold
334 of the HK97 virus²³, some key differences exist. Che8 lacks the G-loop that is found
335 near the C-terminal end of the spine helix in the HK97 phage major capsid protein
336 (Figure 1 A), therefore, Che8 has a continuous spine helix (Figure 2 B). Che8 also lacks
337 the “protein chainmail” of the HK97 phage; the cryo-EM density map revealed that there
338 was no density to suggest isopeptide bond formation, nor were there any amino acids in
339 the correct location to potentially form an isopeptide bond. Unlike Che8, both Bobi and
340 Ogopogo are more similar to HK97. They both contain a G-loop, although they are more
341 extended when compared to the original HK97 fold. Ogopogo additionally has an
342 extended A-loop that extends over the G-loop and makes important stabilizing contacts
343 with the G-loop and spine helix (Figure 2 B, bottom right). The A-loop is in the same
344 position as the A-loop of phage T7 where it was first characterized²⁶; we name this the
345 A₃-loop. Bobi has an additional loop between the A and P domains, in a similar position
346 to the A-pocket described in phage T7²⁶; we name this the A₄-loop. Ogopogo and Che8
347 do not have the A₄-loop. The A₄-loop in Bobi does not make intermolecular interactions
348 with other adjacent major capsid proteins, although it does make some intramolecular
349 hydrogen bonds. However, the A₄-loop is spatially very close to the A₃-loop of an
350 adjacent major capsid protein (discussed in more detail later). Furthermore, both Bobi
351 and Ogopogo have an isopeptide bond, with clear density in the cryo-EM map showing
352 the covalent link between a lysine (Bobi, lysine 70 and Ogopogo lysine 63) in the E-loop

353 and either aspartic acid or asparagine in the P-domain (Bobi, Asp 266 and Ogopogo
354 Asn 283) of the adjacent major capsid protein: this demonstrates that they form the
355 characteristic “protein chainmail” like the original HK97 fold. Ogopogo and Bobi both
356 have an extended P-loop within the P-domain and three of these are found in close
357 contact around the local 3-fold axis of the capsid. These P-loops will be discussed in
358 greater detail later. This structural comparison of the three F1 major capsid protein
359 phamilies suggested that the Che8-like phages may be more divergent from Bobi and
360 Ogopogo.

361
362 For simplicity, from this point on the major capsid protein phams will be called by the
363 corresponding representative phage used in Figure 2; the Che8-like phages (pham
364 4631); the Ogopogo-like phages (pham 57445) and the Bobi-like phages (pham 15199).

365

366 ***The three major capsid protein phamilies of the F1 subcluster constitute two***
367 ***structural groups of major capsid protein in the actinobacteriophages***

368 To confirm the structural observations, we next put the three F1 major capsid protein
369 phamilies into the broader context of the major capsid proteins from the
370 actinobacteriophages database since focusing on just the three F1 phamilies would
371 likely not reveal much insight into their level of evolutionary relationship due to their
372 relatively high structural similarity. We, therefore, created a structural dendrogram of all
373 the major capsid protein phamilies annotated in the actinobacteriophages (Figure 3).
374 Previously, structural comparison of distantly related, yet conserved, protein folds has
375 been used successfully to imply evolutionary links between viral capsid proteins; for

376 example, with the PRD1 and other double jelly-roll viral capsid proteins including
377 adenovirus^{66,70,71}, as well as showing a link between the dsDNA tailed phages and
378 Herpes virus³.

379
380 To create the structural dendrogram we used AlphaFold⁵⁴ to predict the three-
381 dimensional HK97-folds of the major capsid proteins. Folding every major capsid protein
382 in the actinobacteriophage database (over 3000 entries when the analysis was carried
383 out in July 2021) was not feasible from a computational standpoint due to the large
384 number of major capsid proteins. Therefore, we selected a representative major capsid
385 protein from each cluster (139 total clusters at the time of analysis), as well as for every
386 Singleton (62 at the time of analysis), as each Singleton could represent a future cluster
387 distinct from the extant groups. For those clusters (A, BN, CZ, DN, and F) with more
388 than one major capsid protein family, we folded a representative of each major capsid
389 protein family from that cluster. In total, the structure of 201 major capsid proteins
390 were predicted using AlphaFold and represent the forty-two annotated major capsid
391 protein families of the actinobacteriophages.

392
393 We validated a subset of the AlphaFold predictions with cryo-EM derived structures
394 (Supporting Figure 1), revealing excellent agreement for most of the HK97-fold (RMSD
395 values between 0.8 - 1 Ångstrom). While AlphaFold performs well for most of the fold,
396 including the structured A-domain and P-domain, it does not as accurately predict the E-
397 loop, and in most cases, the N-arm is badly predicted (Supporting Figure 2). These
398 results concerning the E loop and N arm are understandable: the N-arm and E-loop

399 make long-range interactions with other major capsid proteins within the capsid and
400 previous studies have shown quite different conformations of the same HK97-fold major
401 capsid protein within its asymmetric unit and during its assembly, showing that both the
402 E-loop and the N-arm are often in different positions and, consequently, hard to predict.

403

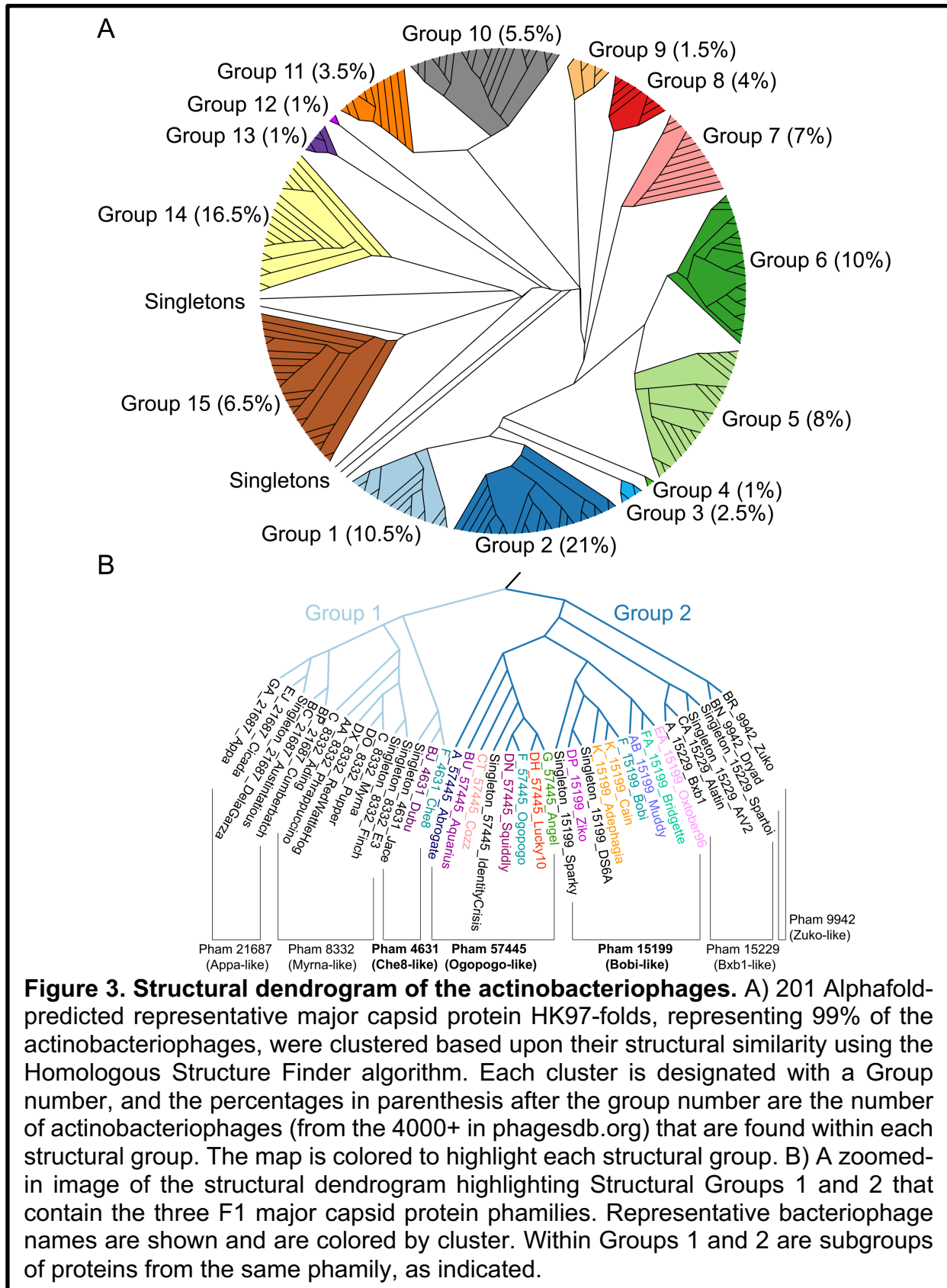
404 All tailed phages use a scaffolding protein domain during capsid assembly to create the
405 empty capsid into which the viral DNA genome is packaged⁷². This scaffolding protein
406 domain can be either an independent protein (called scaffolding protein) or an N-
407 terminal extension of the major capsid protein sequence (called the delta domain) and
408 in phage HK97 is cleaved from the major capsid protein after capsid assembly⁷².

409 Approximately 35% of the Alphafold predicted major capsid proteins from the
410 actinobacteriophages had an N-terminal extension that was similar in size to the HK97
411 phage delta domain. Some of the predicted delta domains in the actinobacteriophage
412 major capsid proteins were almost as large (300 amino acids) as the major capsid
413 protein and it is not possible to predict the cleavage site between the delta domain and
414 the post-cleavage N-arm. We therefore manually truncated all the Alphafold predicted
415 major capsid proteins to remove the N-terminal arm and the delta domain, if present, to
416 make sure that we did not introduce bias from the N-arm and delta domains into the
417 structural comparison. PDB-format files for the 201 full-length and truncated major
418 capsid protein predictions can be found in Supporting Information.

419

420 These 201 truncated major capsid protein predictions were then used to create a major
421 capsid protein structural dendrogram of the actinobacteriophages using the

422 Homologous Structure Finder algorithm⁶⁶ (Figure 3 A). The algorithm compares the
423 three-dimensional Alphafold predictions and classifies the major capsid proteins on their
424 structural similarity. The sophisticated classification methodology allows for the creation
425 of a structural dendrogram whereby common structural elements between the major
426 capsid proteins are identified and a common structural ancestor can be inferred. It has
427 been used successfully for other protein fold lineages^{66,73}. The major advantage of this
428 methodology is for detecting similarities in protein folds even when no similarities
429 remain in the amino acid sequences. The forty-two major capsid protein families
430 within the actinobacteriophages have less than 20% amino acid sequence identity,
431 meaning that comparison of the major capsid protein structures is the best way to reveal
432 similarity and infer evolutionary links between the major capsid proteins.



433 The structural map of the actinobacteriophages revealed that the 42 major capsid

434 protein families can be classified into 15 structural groups (Figure 3 A) that are likely
435 to be evolutionarily related. Each structural group is classified solely on the three-
436 dimensional structure of the major capsid protein and is independent of the cluster and
437 major capsid protein family. Beyond the 15 structural groups are several “structural
438 Singletons”. The structural dendrogram supports the initial structural comparison of the
439 three Cluster F1 phage major capsid proteins in that the Che8-like family, sorted into
440 Group 1, is more diverged from the Ogoogo and Bobi-like families found in Group 2
441 (Figure 3 B). Both groups are relatively large and just over 30% of all the annotated
442 actinobacteriophages use major capsid proteins found in these structural groups (Group
443 1: 10.5% of all annotated actinobacteriophages and Group 2: 21%).

444

445 Group 1 (Supporting Figure 3) contains three different major capsid protein families:
446 4631 (Che8-like), 8332 (Myrna-like), and 21687 (Appa-like). It is very similar to the
447 HK97-fold of the HK97 virus, with RMSDs when compared to the HK97 major capsid
448 protein of between 1 and 1.3 Å. However, all of the Group 1 major capsid proteins lack
449 the G-loop of the spine helix. The Appa-like (21687) sub-group all have a 7-strand beta-
450 sheet in the A domain, compared to the 5-strand sheet of the HK97-virus. The Appa-like
451 members also have a large loop of varying length at the very end of the spine helix. The
452 Myrna-like (pham 8332) sub-group all have a 6-strand beta sheet in the A domain. The
453 Che8-like (pham 4631) sub-group all have the canonical five-strand beta sheet in the A
454 domain but have an extra helix at the top of the A domain and an elongated spine helix
455 with two extra turns when compared to the HK97 spine. All three structural sub-groups
456 are defined by their major capsid protein family with no evidence of a member of a

457 phamily being more closely related to another phamily than its own phamily. For
458 example, no Che8-like major capsid proteins cluster within the Appa-like or Myrna-like
459 structural sub-groups.

460

461 Group 2 (Supporting Figure 4) contains four different major capsid protein phamilies:
462 9942 (Zuko-like), 15229 (Bxb1-like), 15199 (Bobi-like), and 57445 (Ogopogo-like). The
463 main architecture of the HK97-fold of Group 2 is once again highly similar to the HK97-
464 fold of phage HK97, with an RMSD of between 1 and 1.4 Å. The main difference
465 between Group 2 and HK97 is the presence of a larger G-loop within Group 2. The
466 Ogopogo-like (57445) phages all have an elongated A₃-loop within the A-domain
467 directly above the G-loop and the A₃-loop is predicted to interact with the G-loop via
468 hydrogen bonding; this is confirmed by the cryo-EM-derived model of Ogopogo. The
469 Bxb1-like (15229 sub-group) and Bobi-like (151999 sub-group) proteins contain an
470 elongated P-loop in one of the beta-sheets of the P-domain. This loop is typically
471 located at the 3-fold axis of the capsid and suggests that these phages have a raised
472 “turret” at the three-fold. The “turret” can be seen in the cryo-EM maps of the Bobi-like
473 (15229) capsids. The final sub-group, the Zuko-like (9942), are the most distantly
474 related to the other three, although, like the Ogopogo-like sub-group, they have a similar
475 extended A₃-loop.

476

477 ***The Bobi-like (15199) phamily can form differently-sized capsids***

478 Having characterized the three F1 phamilies and shown that Che8 is likely to be
479 evolutionarily distinct from the other two phamilies, we next wanted to investigate how

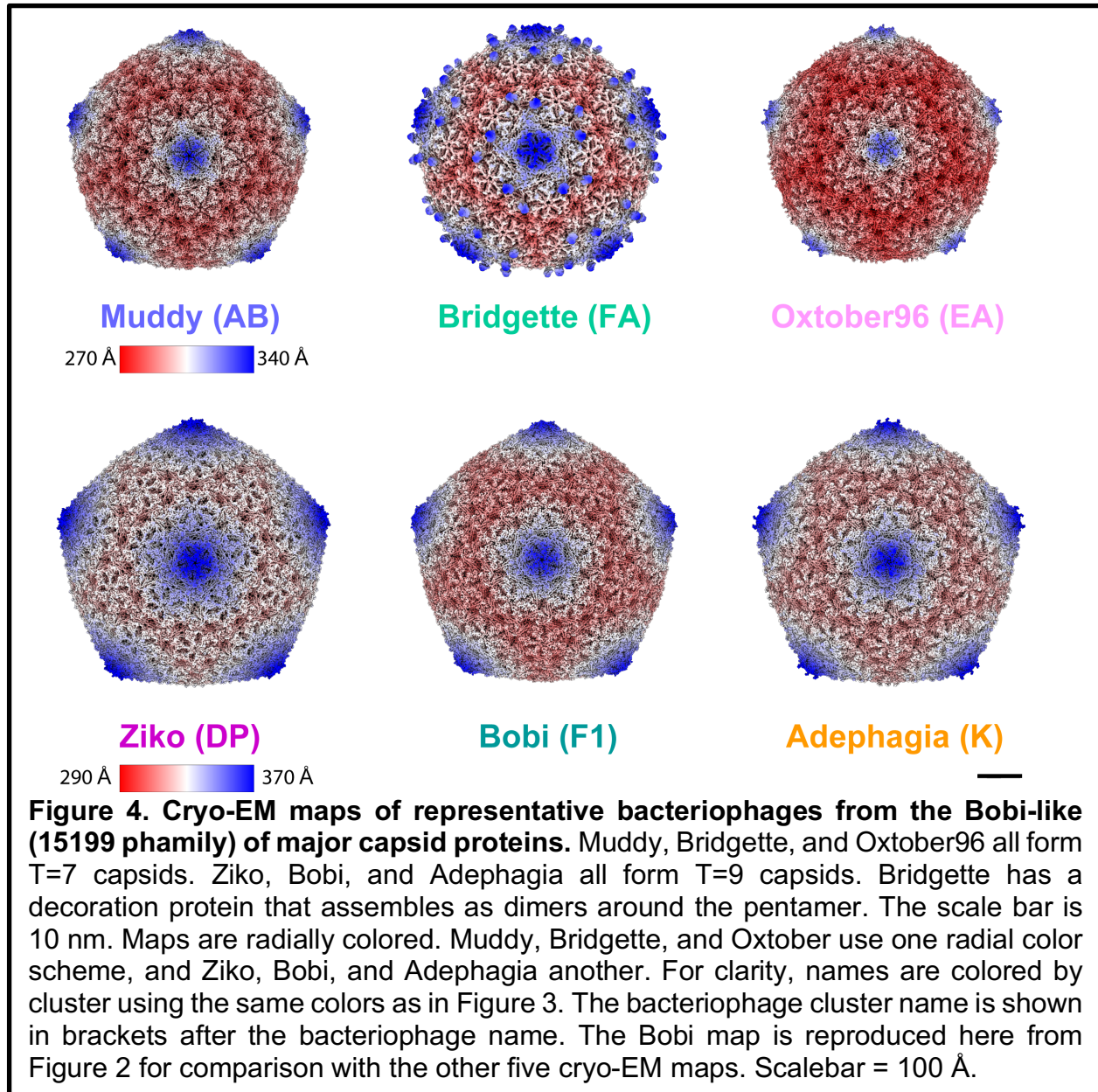
480 the HK97-fold and capsid stability mechanisms are conserved within closely related
481 phages. We chose to concentrate on the Group 2 phages since they use the protein
482 “chainmail” found in HK97. Alignment of all the AlphaFold-predicted major capsid
483 proteins from Group 2 shows lysine and aspartic acid/asparagine at the expected
484 positions in the E-loop and P-domain in the majority of the Group 2 phages, apart from
485 those in the Zuko-like (9942) sub-group and a subset of the Cluster K phages in the
486 Bobi-like (15199) sub-group. Likewise, all the sub-groups, apart from the Zuko-like
487 (9942) have a glutamic acid in a position within the P-domain that could act like the
488 Glu363 in the HK97 major capsid protein for the catalysis of the cross-linking.

489

490 It was surprising to identify some of the K subcluster lacking the lysine residue needed
491 for the isopeptide bond since all the other Bobi-like (15199) phages were predicted to
492 use it. Removal of the isopeptide bond in HK97 by mutating the E-loop lysine to tyrosine
493 results in non-viable phage particles indicating that the isopeptide bond is required⁷⁴ for
494 infectious capsids to be made. The Bobi-like (15199) phages, therefore, provided an
495 opportunity to characterize phage structures with and without the isopeptide bond and
496 investigate how/and if the capsid compensates for its absence. We carried out cryo-EM
497 on five other members of the Bobi-like (15199) phage capsids to yield density maps of <
498 4 Å resolution (Supporting Table 2). We found that some of the Bobi-like (15199)
499 phages formed T=9 capsids while others formed T=7 capsids (Figure 4). In each of the
500 six phages (including Bobi), only the major capsid protein was identified in the cryo-EM
501 map; no minor capsid proteins were observed. Bridgette of Cluster FA, however, did

502 have a decoration protein (Gp7, Supporting Figure 6) that bound as dimers around the
503 5-fold axis of the pentamer, reminiscent of the phi29 phage spike proteins²⁸.

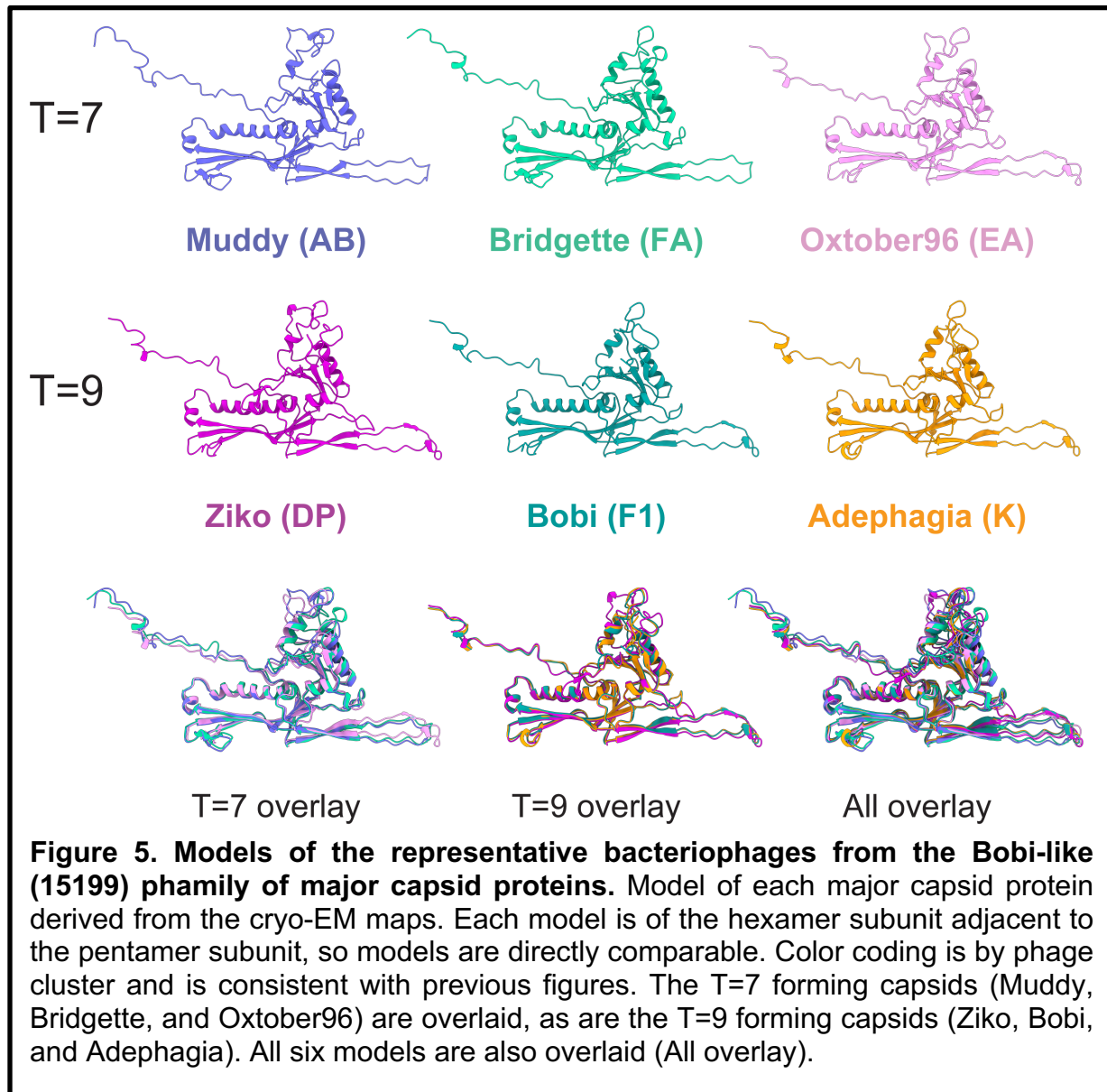
504

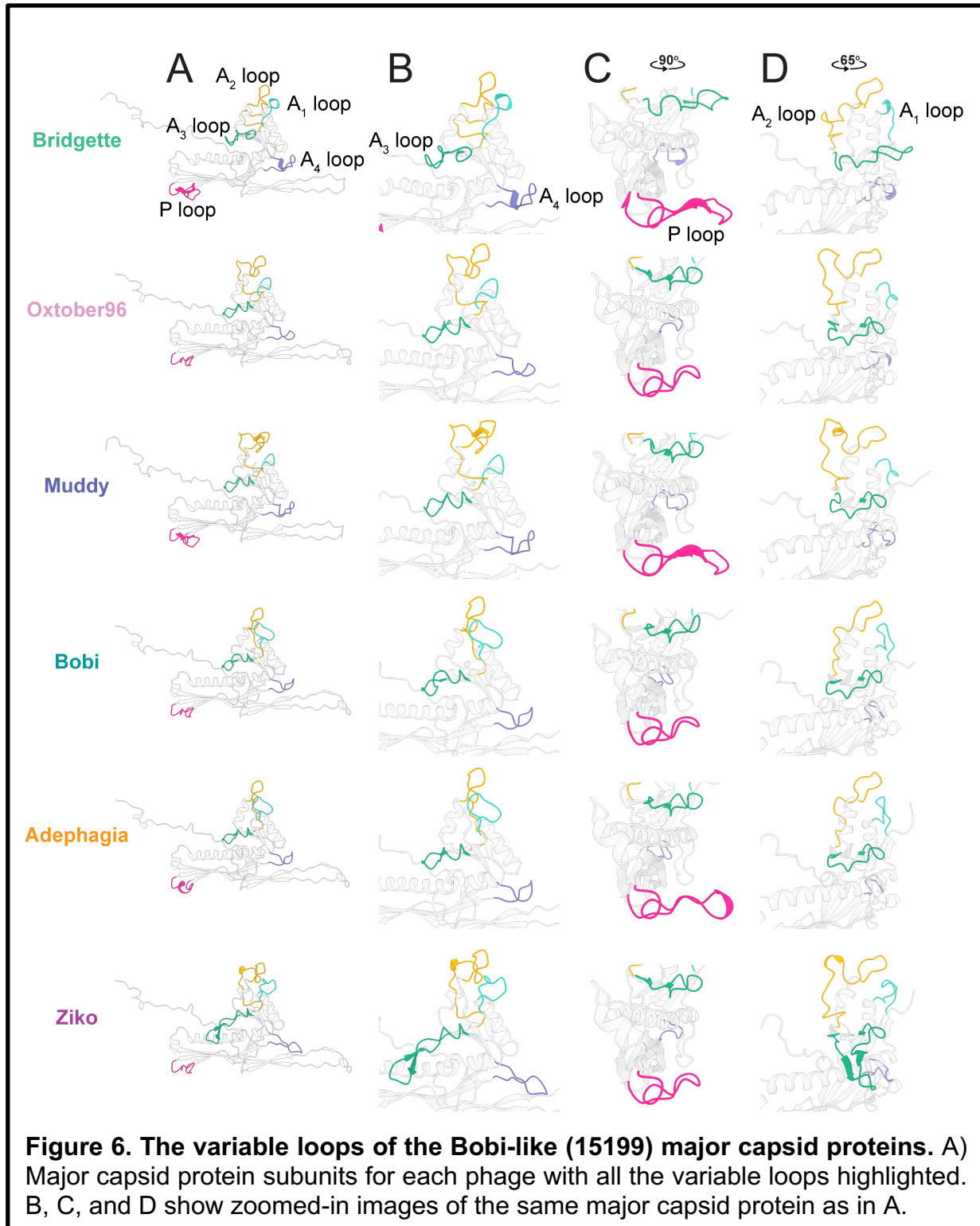


505

506

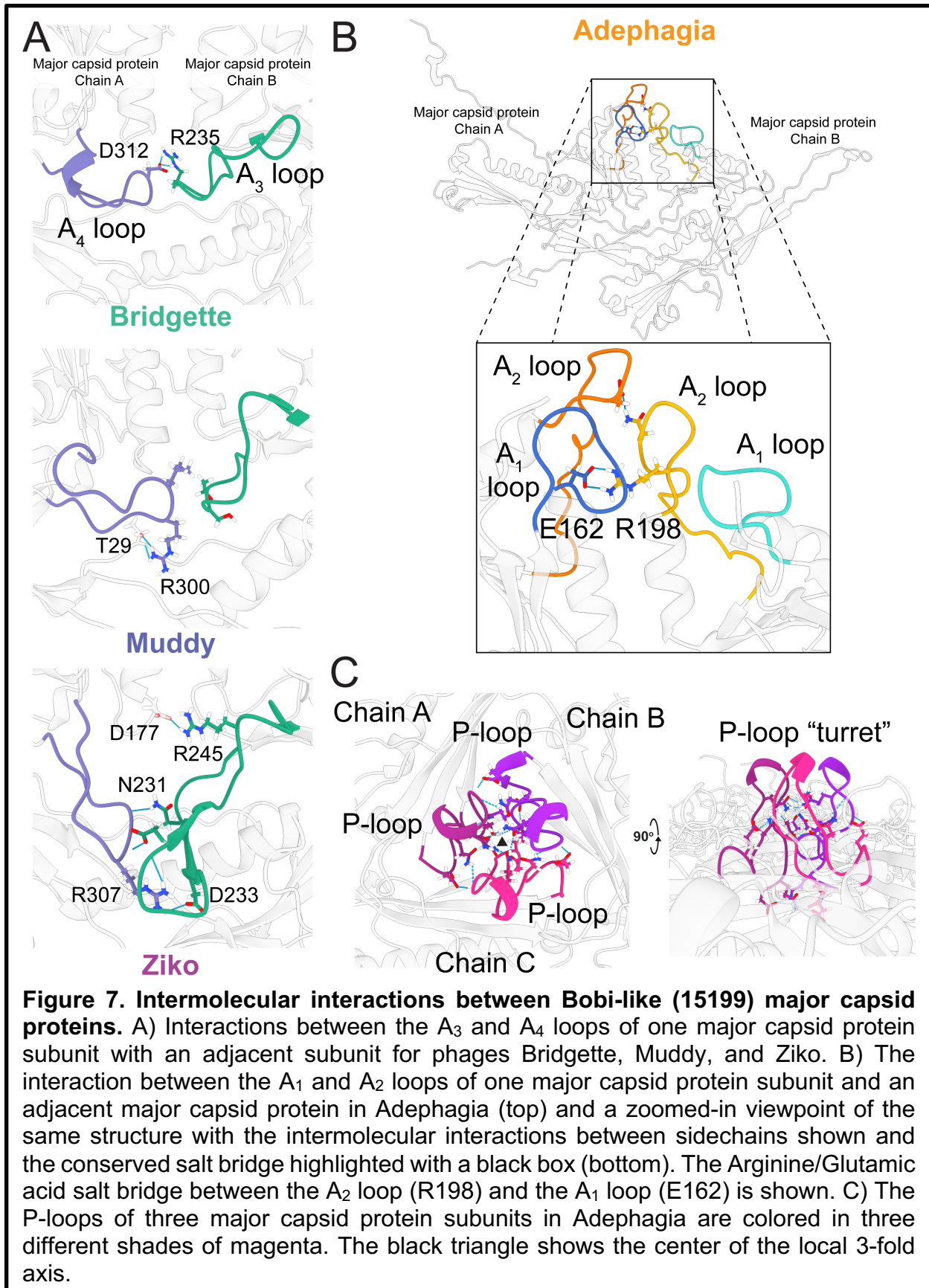
507 **The HK97-folds of the Bobi-like phamily (Pham 15199) are highly**
508 **conserved, but exhibit structural diversity in the loop regions**
509 The high resolution of the six maps of the representative Bobi-like (pham 15199)
510 phages allowed for *de novo* model building of each of the major capsid proteins.
511 Comparison of the HK97-folds showed very high similarity between them (Figure 5),
512 with the highest RMSD value of 1.2 Å (Supporting Table 3). The protein fold is highly





513 conserved and near identical, especially in the secondary structure alpha helices and
514 beta sheets and can be overlaid without much deviation along the protein fold. It is

515 within five loop regions that the most structural diversity is observed (Figure 6). We
516 have designated these loop regions A₁-A₄ because of their position in the A domain, as
517 well as the P-loop found in the P-domain. The A₃ and A₄ loops were first described in
518 the HK97-fold of the phage T7 major capsid protein and named the A-loop (A₃ loop) and
519 A-pocket (A₄ loop)²⁶. We have renamed them here because of the extra loops we have
520 identified. All the structurally characterized Bobi-like (pham 15199) phages have both A₃
521 and A₄ loops. Within Bobi, Oxtober96, and Adephagia, the two loops are of similar
522 length and make intramolecular interactions but do not interact with one another. The
523 other three phages, Bridgette, Muddy, and Ziko, all have increasingly long A₃ and A₄
524 loops, with those of Ziko being the longest (Figure 6 B). The extended A₃ loop in Ziko
525 extends out over its G-loop, reminiscent of the same loop found in the Ogopogo-like
526 phages (Figure 2 B). The G-loop stabilizes the Ziko A₃ loop with a salt bridge involving
527 Gln130 in the G-loop and Asp223 in the A₃ loop. This is not observed in the Ogopogo-
528 like phages where hydrogen bonds are used to stabilize the A₃ loop above the G-loop
529 (Figure 2 B). The extended A₃ and A₄-loops in Bridgette, Muddy, and Ziko stabilize the
530 capsid through intermolecular interactions (Figure 7 A), either forming a single salt
531 bridge (in the case of Bridgette) or a salt bridge combined with hydrogen bonds (in the
532 case of Ziko) between the two loops on neighboring chains. Muddy does not make an
533 intermolecular contact between the A₃ and A₄-loops, instead, the A₄ loop forms a salt
534 bridge with the N-arm of the adjacent major capsid protein. Only a single tryptophan
535 (W224 in Bobi) is conserved in the A₃ loop across the Bobi-like (15199) major capsid
536 proteins. It forms a pi-pi interaction with



538 a conserved phenylalanine (Phe127 in Bobi) that presumably stabilizes the A₃ loop
539 (Supporting Figure 6). No residues are conserved in the A₄ loop.

540

541 Extending this analysis to the wider Structural Group 2 (Figure 3) using the Alphafold
542 predicted models (Supporting Figure 4) suggests that the two Singletons, DS6A and
543 Sparky, both have elongated A₃ and A₄ loops like Ziko but the A₃ loop forms a beta
544 hairpin structure. The A₄ loop is not universal amongst the Group 2 phages (Supporting
545 Figure 4). For example, the Ogotogo-like (57445 phamily) and Bxb1-like (15229
546 phamily) phages, completely lack the A₄ loop although they still have the A₃ loop.

547

548 The A₁ and A₂ loops are found at the top of the A domain (Figure 6 D), with the A₂ loop
549 inserting into the center of the hexamer or pentamer capsomere. Oxtober96, Ziko, and
550 Muddy all have elongated A₂ loops. A comparison of the A₁ and A₂ loops in the context
551 of the capsid (Supporting Figure 7) shows that there is a conserved salt bridge between
552 an Arginine in the A₂ loop of one major capsid protein and a Glutamic acid in the A₁ loop
553 of an adjacent major capsid protein (Figure 7 B). However, in Bridgette, the salt bridge
554 is between the two A₂ loops (Supporting Figure 7). The elongated A₂ loops do not
555 appear to result in a consistent increase in intermolecular or intramolecular interactions
556 between the major capsid proteins (Table 2) and no other amino acids are conserved.

557

Table 2. Hydrogen bonds between the A₁ and A₂ loops. Hydrogen bonds and salt bridges specific to the A₁ and A₂ loops were determined in ChimeraX⁴⁹.

<i>Bacteriophage name</i>	<i>Intermolecular bonds</i>	<i>Intramolecular bonds</i>
<i>Adephagia</i>	3	32
<i>Bobi</i>	5	32
<i>Ziko</i>	6	31
<i>Muddy</i>	8	24
<i>Oxtober96</i>	8	25
<i>Bridgette</i>	4	43

558 The P-loop (Figure 6 C) makes contact with other P loops around the 3-fold axis,
 559 creating small “turrets” that stick outward from the capsid (Figure 7 C). The P-loops
 560 make several hydrogen bonds and salt bridges (Table 3) between adjacent P-loops that
 561 are likely to play a role in the stabilization of the local 3-fold axis. Adephagia has one of
 562 the longest P-loops and makes the most salt bridges and hydrogen bonds between the
 563 P loops out of all six Bobi-like phages.

Table 3. Hydrogen bonds in the local 3-fold axis. Hydrogen bonds and salt bridges specific to the P-loop in a single local 3-fold axis were assessed in ChimeraX⁴⁹. The number of bonds between all the major capsid proteins that are involved in the local 3-fold was determined using PDBsum⁶⁴.

<i>Bacteriophage name</i>	<i>P-loop hydrogen bonds</i>	<i>P-loop salt bridges</i>	<i>3-fold hydrogen bonds</i>	<i>3-fold salt bridges</i>
<i>Adephagia</i>	41	9	207	73
<i>Bobi</i>	18	3	201	90
<i>Ziko</i>	18	3	236	89
<i>Muddy</i>	24	0	273	65
<i>Oxtober96</i>	16	0	246	108
<i>Bridgette</i>	19	3	198	79

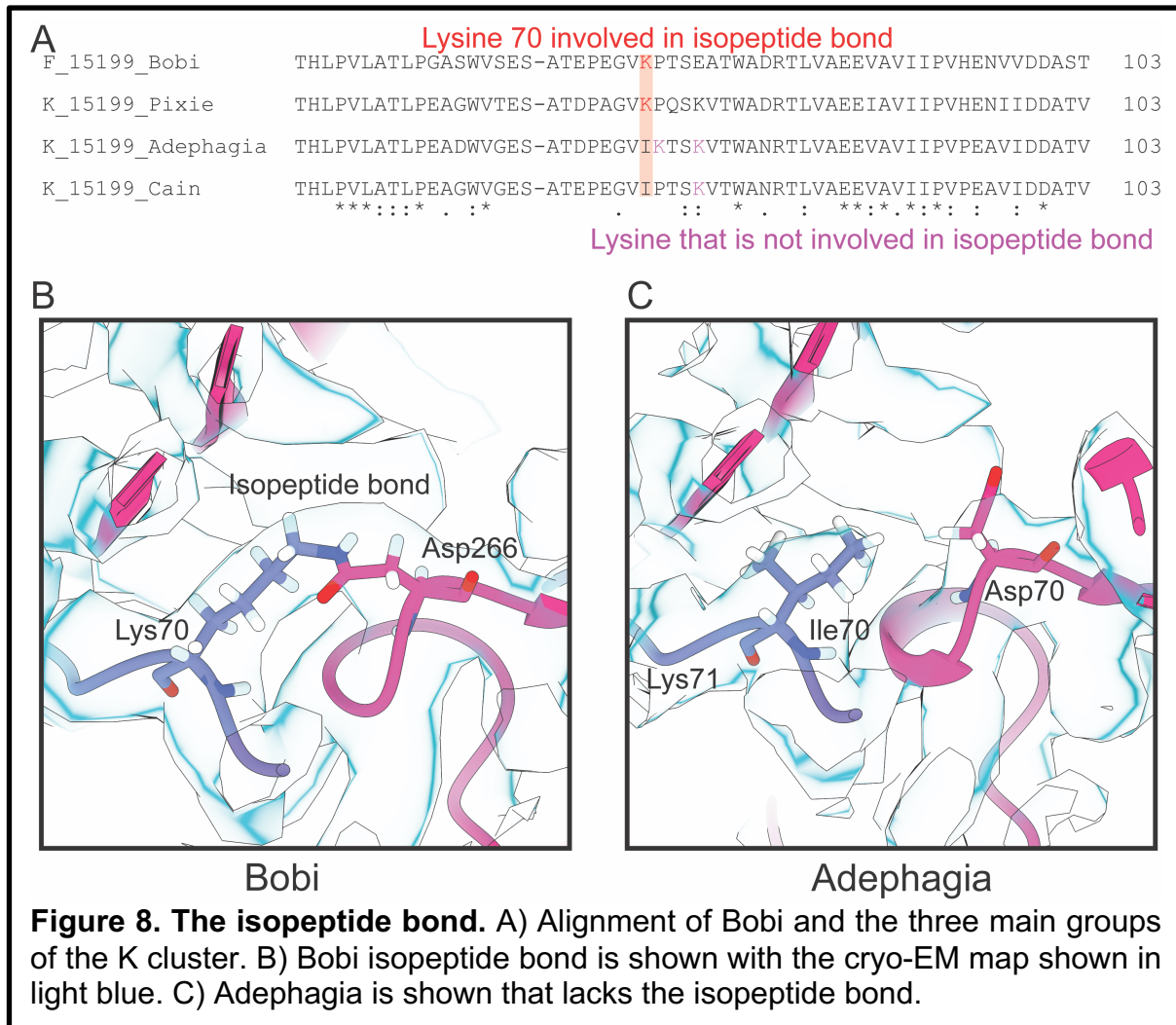
564

565 The G-loop structure is well conserved across all of the Bobi-like (15199) phages and is
566 a clear structural marker for this phamily of phage major capsid proteins despite only
567 having a single conserved glycine and proline across the Bobi-like (15199) major capsid
568 proteins (Supporting Figure 4).

569

570 ***Covalent crosslink residues are not found in all of the Bobi-like major capsid***
571 ***proteins***

572 Alignment of the Bobi-like (15199) phamily major capsid protein amino acid sequences
573 revealed that a subset of the Cluster K phages lack the lysine in the E-loop at position
574 70 of the Bobi major capsid protein. This lysine, present in every other Bobi-like phamily
575 member, as well as most of the Cluster K phages, is half of the amino acid pair that
576 creates the isopeptide bond between two major capsid protein subunits. This lysine is
577 substituted by isoleucine at position 70 (K70I, Figure 9 A) in 48% (78 in total) of the
578 Cluster K phages, with the remaining Cluster K phages having the lysine at the correct
579 position, demonstrating that it is not a rare occurrence. MAFFT alignment and
580 phylogenetic analysis of the major capsid proteins showed that the Cluster K phages
581 (Supporting Figure 8) are most closely related to the Cluster F phages (of which Bobi is
582 the representative) with 70% amino acid sequence identity between Bobi and
583 Adephagia (Clusters F and K, respectively). Within the K70I sub-group of Cluster K
584 phages, there are nearby lysine residues that we hypothesize could act as the lysine for
585 the isopeptide bond. Depending on the position of this misplaced lysine, these Cluster K
586 phages can be divided into two groups (Figure 8 A). We have termed one group the



587 Adephagia-like phages, and the other the Cain-like phages. Both contain the isoleucine
 588 replacement of the isopeptide-forming lysine. However, the Adephagia-like phages have
 589 a lysine adjacent to the isoleucine, while the Cain-like phages have a lysine four
 590 residues downstream (towards the C-terminus) from the isoleucine. The Cain-like
 591 phages are a relatively small group, with only eight members (~5% of the Cluster K
 592 phages). Overall, the major capsid proteins of Adephagia and Cain are highly similar to
 593 the other Cluster K phages with an amino acid sequence identity of 92%. Having
 594 already obtained a high-resolution map of Adephagia (Figure 5), we performed cryo-EM

595 on Cain and obtained a sub 3 Å map (Supporting Figure 9 A) to investigate whether it
596 could form the isopeptide bond with the downstream lysine.

597

598 Analysis of the six cryo-EM maps from the Bobi-like (pham 15199) phages (Figure 4),
599 as well as the map of the Cluster K Cain phage confirmed that all the phages, except
600 Adephagia and Cain, had clear density for the isopeptide bond between the lysine in the
601 E-loop and an aspartic acid in the P-domain of the adjacent major capsid protein (Figure
602 8 B). The lysine residues within Adephagia and Cain that we hypothesized could form
603 the isopeptide bond were therefore found not to be involved in covalent bond formation
604 (Figure 8 C and Supporting Figure 9 B).

605

606 A consequence of the isopeptide bond is that all the major capsid proteins are
607 covalently linked to one another, forming a large complexes. Previous SDS-PAGE
608 analysis of the capsid of the HK97, where the isopeptide bond was first demonstrated
609 (Figure 1), showed that the major capsid protein was unable to enter the gel due to its
610 extensive crosslinking and large size⁷⁵. We, therefore, ran the Ziko (that contains the
611 isopeptide bond) and Adephagia (with no isopeptide bond) capsids on SDS-PAGE
612 (Supporting Figure 10). The gel confirmed the cryo-EM analysis of isopeptide bond
613 formation: no major capsid protein band was observed for Ziko at the expected
614 molecular weight of 34 kDa but instead, there were dark areas at the top of the gel
615 reminiscent of the HK97 SDS-PAGE analysis. Conversely, a large band consistent with
616 the major capsid protein of Adephagia was detected on the gel at approximately 32 kDa
617 (the predicted size of Adephagia gp13 major capsid protein is 32.7 kDa).

618 ***The isopeptide bond catalytic site in the Bobi-like phages is similar to that found***
619 ***in HK97***

620 Phage HK97 was the first (and until now, only) structurally characterized example of the
621 isopeptide bond in the tailed phages; the bond is formed between lysine 169 and
622 asparagine 356 (Figure 1) and has been well characterized. The isopeptide bond has
623 also been shown biochemically in other phages, for example, D3⁷⁶, Q54⁷⁷, and L5⁷⁸ but
624 these have not been structurally characterized.

625

626 The formation of the isopeptide bond is catalyzed by a glutamic acid (Glu363 in HK97)
627 located within a hydrophobic pocket made up of three amino acids (Val163, Met339,
628 and Leu361)²⁴ (Figure 1). The Bobi-like isopeptide bond (Figure 8 B) is similar to that
629 found in HK97; it is formed between lysine 70 in the E-loop and aspartic acid 266 in an
630 adjacent major capsid protein subunit. A highly conserved glutamic acid (Glu86) and
631 valine (Val59) are found in almost identical structural positions as those in HK97.

632 However, there are no equivalent hydrophobic residues in Bobi that would recapitulate
633 the hydrophobic pocket provided by HK97 Met339 and Leu361, suggesting that these
634 residues are not conserved across all phages that use the isopeptide bond and that
635 different ways to create the hydrophobic pocket are possible. All the identified amino
636 acids within the Bobi-like phage catalytic site are highly conserved across all of 15199
637 pham apart from Lysine 70, which is substituted only in the aforementioned subset of
638 the Cluster K phages: the Adephegia-like and Cain-like.

639

640 The catalytic glutamic acid is not structurally conserved across Group 2. In the Bobi-like
641 (15199) sub-group the glutamic acid is structurally conserved (relative to HK97). In the
642 same position within the other members of Group 2, all have a lysine at the same
643 position. The Zuko-like (pham 9942) have no glutamic acid nearby that could play a
644 catalytic role. The remaining members of Group 2 (Ogpogo-like and Bxb1-like) all have
645 a structurally conserved glutamic acid nearby that could play a similar catalytic role. The
646 position is confirmed in the cryo-EM map of Ogpogo with Glu290 in a position to
647 possibly be the catalytic glutamic acid.

648

649 ***Structural groups do not have a conserved hydrogen bond network***

650 The lack of an isopeptide bond in Adephagia and the other Cluster K phages raised the
651 question as to how they compensate for the absence of the covalent isopeptide bond
652 around the local 3-fold axis for capsid stability. Removal of the isopeptide bond in HK97
653 results in unviable capsids, suggesting it is critical for the survival of virion. With no
654 minor capsid protein or other accessory protein to compensate for the loss of the
655 isopeptide bond, we examined the hydrogen bonds and salt bridges around the local 3-
656 fold axis, hypothesizing that there would be an increased number of such interactions
657 around the local 3-fold of Adephagia when compared to Bobi, its closest relative in the
658 Bobi-like (15199) pham. Specifically, we predicted that the P-loops at the center of the
659 3-fold would have increased interactions in Adephagia. Indeed, this is what we
660 observed, with an increase in both salt bridges and hydrogen bonds between the P-
661 loops, with Adephagia having three times the salt bridges and double the number of
662 hydrogen bonds when compared to Bobi (Table 3). This equates to an increase of 240

663 kJ/mol free energy between Adephagia and Bobi at the site of the P-loops, although this
664 must be contrasted with a loss of 1068 kJ/mol in free energy because of the removal of
665 the isopeptide bonds. However, despite the increase in interactions at the P-loop, which
666 is located at the center of the local 3-fold axis, there was no increase in the number of
667 hydrogen bonds and salt bridges between Adephagia and Bobi around the wider local
668 3-fold axis that takes into account all nine interacting major capsid proteins (Table 3 and
669 Supporting Figure 11). We next expanded the analysis to the other members of the
670 Bobi-like (15199) pham, which revealed that all the capsids had similar numbers of
671 hydrogen bonds and salt bridges around the local 3-fold axis but only a handful of these
672 were structurally conserved, with different distribution patterns of the interactions for
673 each phage (Table 3 and Supporting Figure 11). We, therefore, conclude that extra
674 stabilization around the local 3-fold axis is not required to compensate for the missing
675 isopeptide bond in Cain-like and Adephagia-like capsids.

676

677 We next hypothesized that the handful of conserved amino acids found in the Bobi-like
678 (15199) phages that were involved in capsid stability would be conserved across all of
679 Structural Group 2; these phages all had very similar major capsid protein HK97-folds
680 and we predicted they would use similar mechanisms to maintain the stability of the
681 capsid around the local 3-fold. However, analysis of the amino acid sequences of the
682 major capsid proteins of Structural Group 2 revealed almost no conserved amino acid
683 sequence identify. A single conserved aspartic acid (D122 in Bobi) is found in all of
684 Structural Group 2, located at the top of the spine helix (C-terminal end). In Bobi (and
685 the other Bobi-like phages that we structurally characterized) this aspartic acid makes a

686 hydrogen bond with the N-arm of the same major capsid protein chain. The hydrogen
687 bond donor amino acid in Bobi is serine (S29), which is common across the majority of
688 Structural Group 2. Some lack the serine and have either lysine or alanine in its place.
689 Ziko is one such phage, which has a lysine at the equivalent position. In Ziko, the
690 conserved aspartic acid interacts with the protein backbone of the lysine in the N-arm in
691 a structurally equivalent position to serine 29 in Bobi.

692

693 Due to the lack of amino acid sequence identity, we turned to the models we had
694 derived from the cryo-EM maps of the phages. We examined the structurally conserved
695 interactions across Structural Group 2, once again hypothesizing that the most critical of
696 these interactions would be conserved. We overlaid the local 3-fold axis of all six of the
697 Bobi-like (pham 15199) phages and Ogotogo (pham 57445). To better represent more
698 members of Structural Group 2 in this analysis we also included Cozz, a close relative
699 of Ogotogo and also part of the 57445 pham (Supporting Figure 11). Cozz was
700 subjected to cryo-EM analysis and a sub-3 Å resolution map was obtained that allowed
701 for *de novo* model building. This structural comparison showed that there were no salt
702 bridges conserved between the different phages in Structural Group 2, nor was there a
703 conserved hydrogen bond network. Each phage used a different pattern of bond
704 formation between the major capsid proteins for intermolecular stability. We, therefore,
705 conclude that what unifies a Structural Group is the capsid configuration and that the
706 phages have evolved different bond networks to achieve the same final product.

707

708

709 **Discussion**

710

711 ***Capsid stability***

712 Tailed phages have been found in a wide range of environmental habitats, ranging from
713 relatively benign soil to hot springs and stomach acid²⁷. In addition to these harsh
714 external environments, the capsid is also under stress from the inside: the predicted
715 pressure that the packaged dsDNA exerts on the inside of the capsid has been
716 estimated at 30 atmospheres⁷⁹. The phage capsid must be stable enough to survive
717 these two main stresses. Many stabilization mechanisms have been characterized at
718 the local three-fold axis of the capsid, implying they play an important role. These
719 typically include many inter-capsomer interactions, for example, the interaction of the P-
720 domains around the three-fold axis of the capsid; the N-arm reaching across to make
721 contacts with adjacent major capsid proteins, and the E-loop interacting with the P-
722 domain. Only HK97 has had its isopeptide bond structurally characterized, although
723 phages have been shown to use the isopeptide bond biochemically. Since then, each
724 structurally characterized phage has been found to lack the isopeptide bond but uses
725 alternate mechanisms to compensate for the lack of this bond to stabilize the local
726 three-fold axis. These include extra domains in the HK97-fold, for example, the I
727 domains found in P22³⁹ and T4⁴⁸, that have been shown to play a role in capsid
728 stability⁸⁰. Additional capsid proteins have also been characterized that are thought to
729 play a role in stability. This includes minor capsid proteins/cement proteins found in
730 several tailed phages and which form trimers/dimers throughout the capsid between the
731 hexamers and pentamers. Other proteins, called decoration or ancillary proteins, have

732 also been characterized that may be involved in stability, although in many cases they
733 are not vital for capsid viability (for example, the soc protein of T4⁸¹). Finally, more
734 diverse mechanisms have been characterized such as the lasso-like interactions in the
735 E-loop observed in two phages isolated in hot springs^{40,41}.

736

737 However, some phages, for example, T7²⁶ and the recently structurally characterized
738 phage phiRSA1²⁷, show that some phages rely solely on the electrostatic and
739 hydrophobic interactions between the major capsid proteins²⁷. Here, we have described
740 a similar lack of stabilizing mechanisms in the T=9 actinobacteriophage Che8, which is
741 an even more simplified example of the HK97-fold than phiRSA1; Che8 lacks the
742 isopeptide bond and any other previously characterized capsid stabilizing interactions,
743 instead relying on only a handful of protein: protein interactions between the major
744 capsid proteins that are found in every HK97-fold major capsid protein. The Che8 major
745 capsid protein also lacks the G-loop, which has been shown to play an important role in
746 capsid assembly⁸². Furthermore, it lacks any potential loop that could compensate for
747 the G-loop, demonstrating that the roles of the G-loop in the HK97 capsid are not
748 required across all other HK97-folds. Additionally, Che8 has no minor capsid proteins,
749 decoration proteins, or I-loops/other extended loops or embellishments that may
750 contribute to capsid stability. This suggests that the core HK97-fold is all that is needed
751 for capsid stabilization and that Che8 is likely to be more similar to the earliest HK97-
752 fold. This is further supported by the Structural Group 9 phages that all have relatively
753 small genomes (< 30 kbp) and are predicted to form T=4 or smaller capsids
754 (unpublished data). All of these phages lack a G-loop and are similar in structure to the

755 Che8 HK97-fold with a long spine helix. This leads us to speculate that the earliest
756 common ancestor to these phages lacked the G-loop. It also suggests different
757 assembly mechanisms between the different HK97-folds since the G-loop in HK97 was
758 shown to play an important role in assembly and mutations in the G-loop led to the
759 formation of aberrant particles⁸².

760

761 The isopeptide bond is a covalent bond between two neighboring major capsid protein
762 subunits and is critical to the viability of HK97 virions. Here, we have structurally
763 characterized other tailed phages that also use the isopeptide bond in their capsid. The
764 Bobi-like (pham 15199) phages all use the same isopeptide bond as in HK97, although
765 they substitute asparagine for aspartate in the P-domain to create the bond. The use of
766 an aspartic acid to form the isopeptide bond has not been observed in the tailed phages
767 before but has been characterized in bacterial proteins⁸³. Also, the mechanism by which
768 the isopeptide is formed may be subtly different. The catalytic glutamic acid residue is
769 still present in the Bobi-like phages, but they lack two of the residues known to form the
770 hydrophobic pocket that is important for the catalysis of the bond²⁴. There are no
771 obvious analogs in the Bobi-like phages for those two residues, and these phages may
772 create the hydrophobic pocket through other means. However, not all of the Bobi-like
773 phages use the isopeptide bond; a small subset of the Cluster K phages, which we term
774 the Adephagia and Cain-like phages, do not use the isopeptide bond and the lysine in
775 the E-loop is substituted with isoleucine. This resulting residue chemistry prevents the
776 formation of an isopeptide bond. Phylogenetic analysis of the Bobi-like phages
777 (Supporting Figure 8) suggests that the Cluster K phages diverged from within the Bobi-

778 like phamily. Although this is speculative, it does support the model that the Adephagia-
779 like and Cain-like phages had the isopeptide bond at some point before it was lost, as
780 opposed to being an intermediate between non-isopeptide bond phages that then
781 evolved to have the isopeptide bond. This is further supported by the other Cluster K
782 phages having the correct lysine for isopeptide formation and presumably forming that
783 isopeptide bond. We were unable to identify any unique increase in inter-capsid
784 interactions in the Adephagia- and Cain-like phages that would compensate for the loss
785 of the isopeptide bond. This suggests that, at least in the Bobi-like phages, the
786 isopeptide bond is not critical to the viability of the phage capsid and that compensatory
787 mechanisms, for example, minor capsid proteins, are not needed. This raises the
788 question as to the role of the isopeptide bond, and why some phages do not require the
789 extra stabilization it affords. A potential explanation is that Cain- and Adephagia-like
790 phages package less dsDNA, exerting less internal pressure on the capsid than those
791 that use the isopeptide bond. However, this correlation cannot yet be made as the
792 amount of dsDNA packaged has not been measured, although we observe that both
793 phages have cos-type genome ends that typically means that the DNA packaged is the
794 same as the genome length.

795

796 ***Capsid size***

797 The tailed phages make protein shells of variable sizes. The smallest to date are the
798 T=4 capsids of P68³⁰ and the T=3 prolate phi29²⁸. The majority are predicted to be T=7,
799 although many “jumbo” phages have been characterized with very large T numbers³².
800 How capsid size is controlled is still an open question. However, many major capsid

801 protein mutants that change the size of the final capsid have been identified in the
802 model phages P22 and T4. The major capsid protein mutants in P22, where the capsid
803 protein is referred to as the coat protein, all result in the wild-type T=7 capsid with the
804 ability of also creating smaller T=4 capsids or aberrant particles⁸⁴. Within the prolate
805 phage T4, the mutants result in “giant” capsids that have lost the ability to regulate the
806 length of the prolate caps and form very long prolate heads⁸⁵. The work on
807 *Staphylococcus aureus* infecting phages and the mechanisms that this bacterium uses
808 to co-opt the phage capsids for the use of the bacteria all result in smaller capsids^{45,34}.
809 Here we have identified several closely related phages that use related major capsid
810 proteins from that same protein phamily, but make either T=7 or T=9 capsids. There are
811 no obvious differences in structure or amino acid conservation between these T=9 and
812 T=7 phage capsids (from phamily 15199) that explains the difference in size. The T=7
813 capsids use a different phamily of scaffold proteins than the T=9. supporting the role of
814 the different scaffolding proteins as the main mechanism of capsid size determination.
815 However, further work is needed to characterize the mechanisms by which these
816 phages assemble. The actinobacteriophages are a rich resource for these types of
817 studies. For example, the structural Group 1 phages contain both Che8 (a T=9 capsid)
818 and Myrna, a T=16 capsid that uses minor capsid proteins⁵¹. Further study of the Group
819 1 phages could provide important insights into how minor capsid proteins are first
820 incorporated into the capsid and how larger capsids evolve.

821

822

823

824 ***The evolution of the major capsid proteins of the actinobacteriophages***

825 We have reported here the first systematic structural study of a group of phages that
826 infect hosts from a single phylum of bacteria. The actinobacteriophages infect hosts
827 from an important bacterial phylum, with *Mycobacterium tuberculosis* a major health
828 concern around the world and non-tuberculosis mycobacteria a major source of lung
829 disease. Most phages are specific to a single host, although some can infect and
830 replicate within many species of the same phylum. There are likely several reasons for
831 the limited host range, including specificity of host binding proteins in phages, codon
832 usage, differences in cellular machinery, and presence of phage-resistance
833 mechanisms⁸⁶. Phages are very likely to be limited to a specific phylum and to our
834 knowledge presently there are no examples of phages that infect hosts in multiple
835 bacterial phyla. The Actinobacteria are an ancient bacterial phylum and are estimated to
836 have diverged from the Proteobacteria phylum over 3 billion years ago⁸⁷. The majority of
837 the well-characterized model system phages infect hosts in the Proteobacteria phylum,
838 for example, P22 that infects *Salmonella* and T4 that infects *E.coli*, and most of the
839 structures of tailed phages come from the Proteobacteria. The temporal distance
840 between the Actinobacteria and Proteobacteria phyla, as well as the lack of evidence of
841 phages moving between phyla, would suggest that the phages that replicate in the two
842 phyla should also be temporally distant and that major capsid proteins will have had
843 different evolutionary pathways. However, the structural analysis of the
844 actinobacteriophages does provide evidence that these phages are ancient. The
845 isopeptide bond in the Bobi-like phages provides some evidence that these HK97-folds
846 predate the divergence of the Proteobacteria and Actinobacteria. Interestingly, it

847 appears that structurally-related major capsid proteins can be found in different capsid
848 morphologies. For example, Structural Group 1 from the actinobacteriophage structural
849 dendrogram contains both the *Siphoviridae* Che8 and *Myoviridae* Myrna, both of which
850 we have structurally characterized in this paper and previously⁵¹. How these two
851 morphologies ended up using the same major capsid protein is intriguing, and additional
852 characterization of Group 1 is needed to explore this further. Is there a T=9 *Myoviridae*
853 in Group 1 that has the same capsid protein structure as Che8? We expect that further
854 research into the different structural groups will provide a deeper insight into the
855 evolutionary relationship between tailed phages.

856 **Acknowledgments**

857

858 We thank Dr. Gabrielle Valles for a helpful review of the paper. We acknowledge the
859 hard work and dedication of all those involved (those at the University of Pittsburgh and
860 HHMI) in the creation and continued support of the SEA-PHAGES program.

861 Specifically, we thank the following students from the SEA-PHAGES program for the
862 isolation of each phage:

863

864 Bridgette: Kira Zack and others at the University of Pittsburgh, PHIRE Program

865 Muddy: Lilli Hoist and others at the University of Kwazulu-Natal, PHIRE Program

866 Oxtober96: Lijia Xin and others at the University of Connecticut, SEA-PHAGES

867 Program

868 Ziko: Anna Bondonese and others at the University of Pittsburgh, SEA-PHAGES

869 Program

870 Bobi: Margaret Korty and Stephanie Maas and others at Purdue University, SEA-

871 PHAGES Program

872 Adephagia: Jordan L. Mosier and others at the University of North Texas, SEA-

873 PHAGES Program

874 Cain: Thomas Cast and Kara Gallo and others at Gonzaga University, SEA-PHAGES

875 Program

876 Che8: V. Kumar and others at the Albert Einstein College of Medicine

877 Ogotogo: Kaylee Nicholson and others at the University of California, Santa Cruz, SEA-

878 PHAGES Program

879 Cozz: Matthew Montgomery and others at the University of Pittsburgh, PHIRE Program

880

881 We also want to thank the myriad of students and faculty who have contributed to the

882 201 phages we included in our bioinformatic analyses.

883

884 A portion of this research was supported by NIH grant U24GM129547 and performed at

885 the PNCC at OHSU and accessed through EMSL (grid.436923.9), a DOE Office of

886 Science User Facility sponsored by the Office of Biological and Environmental
887 Research.

888

889 This work was supported by National Institutes of Health grants GM131729 and Howard
890 Hughes Medical Institute grants GT12053 (to GFH). The University of Pittsburgh Titan
891 Krios microscope and Falcon 3 camera were supported by the Office of the Director,
892 National Institutes of Health, under award numbers S10 OD025009 and S10
893 OD019995, respectively (JFC).

894

895 We also thank the following scientists at PNCC for the data collection: Theo
896 Humphreys, Omar Davulcu, Nancy Meyer, and Rose Marie Haynes.

897

898 **Competing Interests:** G.F.H. is a compensated consultant for Tessera and for Janssen
899 Inc. The remaining authors declare no competing interests.

900 **References**

- 901 1. Helgstrand, C. *et al.* The Refined Structure of a Protein Catenane: The HK97 Bacteriophage
902 Capsid at 3.44Å Resolution. *Journal of Molecular Biology* **334**, 885–899 (2003).
- 903 2. Pietilä, M. K. *et al.* Structure of the archaeal head-tailed virus HSTV-1 completes the HK97
904 fold story. *Proc Natl Acad Sci U S A* **110**, 10604–10609 (2013).
- 905 3. Dai, X. & Zhou, Z. H. Structure of the herpes simplex virus 1 capsid with associated
906 tegument protein complexes. *Science* **360**, eaao7298 (2018).
- 907 4. Sutter, M. *et al.* Structural basis of enzyme encapsulation into a bacterial
908 nanocompartment. *Nat. Struct. Mol. Biol.* **15**, 939–947 (2008).
- 909 5. Nichols, R. J., Cassidy-Amstutz, C., Chaijarasphong, T. & Savage, D. F. Encapsulins: molecular
910 biology of the shell. *Critical Reviews in Biochemistry and Molecular Biology* **52**, 583–594
911 (2017).
- 912 6. Suttle, C. A. Marine viruses — major players in the global ecosystem. *Nat Rev Microbiol* **5**,
913 801–812 (2007).
- 914 7. Jordan, T. C. *et al.* A Broadly Implementable Research Course in Phage Discovery and
915 Genomics for First-Year Undergraduate Students. *mBio* **5**, e01051-13.
- 916 8. Teaching Scientific Inquiry. <https://www.science.org/doi/10.1126/science.1136796>.
- 917 9. Hatfull, G. F. Actinobacteriophages: Genomics, Dynamics, and Applications. *Annual Review*
918 *of Virology* **7**, 37–61 (2020).
- 919 10. Dedrick, R. M. *et al.* Engineered bacteriophages for treatment of a patient with a
920 disseminated drug-resistant *Mycobacterium abscessus*. *Nat Med* **25**, 730–733 (2019).

- 921 11. Diacon, A. H. *et al.* Mycobacteriophages to Treat Tuberculosis: Dream or Delusion?
922 *Respiration* **101**, 1–15 (2022).
- 923 12. Duda, R. L. & Teschke, C. M. The amazing HK97 fold: versatile results of modest differences.
924 *Current Opinion in Virology* **36**, 9–16 (2019).
- 925 13. Suhanovsky, M. M. & Teschke, C. M. Nature’s favorite building block: Deciphering folding
926 and capsid assembly of proteins with the HK97-fold. *Virology* **479–480**, 487–497 (2015).
- 927 14. Zhou, Z. H. & Chiou, J. Protein chainmail variants in dsDNA viruses. *AIMS Biophys* **2**, 200–
928 218 (2015).
- 929 15. Caspar, D. L. & Klug, A. Physical principles in the construction of regular viruses. *Cold Spring*
930 *Harb. Symp. Quant. Biol.* **27**, 1–24 (1962).
- 931 16. Gertsman, I., Fu, C.-Y., Huang, R., Komives, E. A. & Johnson, J. E. Critical Salt Bridges Guide
932 Capsid Assembly, Stability, and Maturation Behavior in Bacteriophage HK97. *Mol Cell*
933 *Proteomics* **9**, 1752–1763 (2010).
- 934 17. Evilevitch, A. *et al.* Effects of Salt Concentrations and Bending Energy on the Extent of
935 Ejection of Phage Genomes. *Biophysical Journal* **94**, 1110–1120 (2008).
- 936 18. São-José, C., de Frutos, M., Raspaud, E., Santos, M. A. & Tavares, P. Pressure Built by DNA
937 Packing Inside Virions: Enough to Drive DNA Ejection in Vitro, Largely Insufficient for
938 Delivery into the Bacterial Cytoplasm. *Journal of Molecular Biology* **374**, 346–355 (2007).
- 939 19. Kindt, J., Tzlil, S., Ben-Shaul, A. & Gelbart, W. M. DNA packaging and ejection forces in
940 bacteriophage. *PNAS* **98**, 13671–13674 (2001).

- 941 20. Lander, G. C. *et al.* Bacteriophage lambda stabilization by auxiliary protein gpD: timing,
942 location, and mechanism of attachment determined by cryoEM. *Structure* **16**, 1399–1406
943 (2008).
- 944 21. Wang, C., Zeng, J. & Wang, J. Structural basis of bacteriophage lambda capsid maturation.
945 *Structure* (2022) doi:10.1016/j.str.2021.12.009.
- 946 22. Zhang, X. *et al.* A new topology of the HK97-like fold revealed in Bordetella bacteriophage
947 by cryoEM at 3.5 Å resolution. *eLife* **2**, e01299 (2013).
- 948 23. Wikoff, W. R. *et al.* Topologically Linked Protein Rings in the Bacteriophage HK97 Capsid.
949 *Science* **289**, 2129–2133 (2000).
- 950 24. Tso, D., Peebles, C. L., Maurer, J. B., Duda, R. L. & Hendrix, R. W. On the catalytic mechanism
951 of bacteriophage HK97 capsid crosslinking. *Virology* **506**, 84–91 (2017).
- 952 25. Huet, A., Duda, R. L., Boulanger, P. & Conway, J. F. Capsid expansion of bacteriophage T5
953 revealed by high resolution cryoelectron microscopy. *PNAS* **116**, 21037–21046 (2019).
- 954 26. Guo, F. *et al.* Capsid expansion mechanism of bacteriophage T7 revealed by multistate
955 atomic models derived from cryo-EM reconstructions. *PNAS* **111**, E4606–E4614 (2014).
- 956 27. Effantin, G., Fujiwara, A., Kawasaki, T., Yamada, T. & Schoehn, G. High Resolution Structure
957 of the Mature Capsid of Ralstonia solanacearum Bacteriophage φRSA1 by Cryo-Electron
958 Microscopy. *Int J Mol Sci* **22**, 11053 (2021).
- 959 28. Xu, J., Wang, D., Gui, M. & Xiang, Y. Structural assembly of the tailed bacteriophage φ29.
960 *Nat Commun* **10**, 2366 (2019).

- 961 29. Aksyuk, A. A. *et al.* Structural investigations of a Podoviridae streptococcus phage C1,
962 implications for the mechanism of viral entry. *Proc Natl Acad Sci U S A* **109**, 14001–14006
963 (2012).
- 964 30. Hrebík, D. *et al.* Structure and genome ejection mechanism of Staphylococcus aureus phage
965 P68. *Science Advances* **5**, eaaw7414 (2019).
- 966 31. Gonzalez, B. *et al.* Phage G structure at 6.1 Å resolution, condensed DNA, and host identity
967 revision to a Lysinibacillus. *J Mol Biol* **432**, 4139–4153 (2020).
- 968 32. Hua, J. *et al.* Capsids and Genomes of Jumbo-Sized Bacteriophages Reveal the Evolutionary
969 Reach of the HK97 Fold. *mBio* **8**, (2017).
- 970 33. Nováček, J. *et al.* Structure and genome release of Twort-like Myoviridae phage with a
971 double-layered baseplate. *Proc Natl Acad Sci USA* **113**, 9351–9356 (2016).
- 972 34. Dearborn, A. D. *et al.* Competing scaffolding proteins determine capsid size during
973 mobilization of Staphylococcus aureus pathogenicity islands. *eLife* **6**, e30822 (2017).
- 974 35. Cui, N. *et al.* Capsid Structure of Anabaena Cyanophage A-1(L). *Journal of Virology* **95**,
975 e01356-21.
- 976 36. Baker, M. L. *et al.* Validated near-atomic resolution structure of bacteriophage epsilon15
977 derived from cryo-EM and modeling. *PNAS* **110**, 12301–12306 (2013).
- 978 37. Kamiya, R. *et al.* Acid-stable capsid structure of Helicobacter pylori bacteriophage KHP30 by
979 single-particle cryoelectron microscopy. *Structure* (2021) doi:10.1016/j.str.2021.09.001.
- 980 38. Jin, H. *et al.* Capsid Structure of a Freshwater Cyanophage Siphoviridae Mic1. *Structure* **27**,
981 1508-1516.e3 (2019).

- 982 39. Hryc, C. F. *et al.* Accurate model annotation of a near-atomic resolution cryo-EM map. *PNAS*
983 **114**, 3103–3108 (2017).
- 984 40. Bayfield, O. W. *et al.* Cryo-EM structure and in vitro DNA packaging of a thermophilic virus
985 with supersized T=7 capsids. *PNAS* **116**, 3556–3561 (2019).
- 986 41. Stone, N. P., Demo, G., Agnello, E. & Kelch, B. A. Principles for enhancing virus capsid
987 capacity and stability from a thermophilic virus capsid structure. *Nat Commun* **10**, 4471
988 (2019).
- 989 42. Johnson, M. C. *et al.* Structure, proteome and genome of Sinorhizobium meliloti phage
990 ΦM5: A virus with LUZ24-like morphology and a highly mosaic genome. *Journal of*
991 *Structural Biology* **200**, 343–359 (2017).
- 992 43. Liu, X. *et al.* Structural changes in a marine podovirus associated with release of its genome
993 into Prochlorococcus. *Nat Struct Mol Biol* **17**, 830–836 (2010).
- 994 44. Bárdy, P. *et al.* Structure and mechanism of DNA delivery of a gene transfer agent. *Nat*
995 *Commun* **11**, 3034 (2020).
- 996 45. Hawkins, N. C., Kizziah, J. L., Penadés, J. R. & Dokland, T. Shape shifter: redirection of
997 prolate phage capsid assembly by staphylococcal pathogenicity islands. *Nat Commun* **12**,
998 6408 (2021).
- 999 46. Zhao, H. *et al.* Structure of a headful DNA-packaging bacterial virus at 2.9 Å resolution by
1000 electron cryo-microscopy. *PNAS* **114**, 3601–3606 (2017).
- 1001 47. Gipson, P. *et al.* Protruding knob-like proteins violate local symmetries in an icosahedral
1002 marine virus. *Nat Commun* **5**, 4278 (2014).

- 1003 48. Chen, Z. *et al.* Cryo-EM structure of the bacteriophage T4 isometric head at 3.3-Å resolution
1004 and its relevance to the assembly of icosahedral viruses. *PNAS* **114**, E8184–E8193 (2017).
- 1005 49. Wang, Z. *et al.* Structure of the Marine Siphovirus TW1: Evolution of Capsid-Stabilizing
1006 Proteins and Tail Spikes. *Structure* **26**, 238-248.e3 (2018).
- 1007 50. Hardy, J. M. *et al.* The architecture and stabilisation of flagellotropic tailed bacteriophages.
1008 *Nat Commun* **11**, 3748 (2020).
- 1009 51. Podgorski, J. *et al.* Structures of Three Actinobacteriophage Capsids: Roles of Symmetry and
1010 Accessory Proteins. *Viruses* **12**, 294 (2020).
- 1011 52. Tivol, W. F., Briegel, A. & Jensen, G. J. An Improved Cryogen for Plunge Freezing. *Microsc*
1012 *Microanal* **14**, 375–379 (2008).
- 1013 53. Zivanov, J. *et al.* New tools for automated high-resolution cryo-EM structure determination
1014 in RELION-3. *eLife* **7**, e42166 (2018).
- 1015 54. Jumper, J. *et al.* Highly accurate protein structure prediction with AlphaFold. *Nature* **596**,
1016 583–589 (2021).
- 1017 55. Goddard, T. D. *et al.* UCSF ChimeraX: Meeting modern challenges in visualization and
1018 analysis. *Protein Sci.* **27**, 14–25 (2018).
- 1019 56. Emsley, P., Lohkamp, B., Scott, W. G. & Cowtan, K. Features and development of *Coot*. *Acta*
1020 *Crystallogr D Biol Crystallogr* **66**, 486–501 (2010).
- 1021 57. Clarke, O. Coot-trimmings. <https://github.com/olibclarke/coot-trimmings>.
- 1022 58. Liebschner, D. *et al.* Macromolecular structure determination using X-rays, neutrons and
1023 electrons: recent developments in Phenix. *Acta Cryst D* **75**, 861–877 (2019).

- 1024 59. Croll, T. I. ISOLDE: a physically realistic environment for model building into low-resolution
1025 electron-density maps. *Acta Cryst D* **74**, 519–530 (2018).
- 1026 60. Russell, D. A. & Hatfull, G. F. PhagesDB: the actinobacteriophage database. *Bioinformatics*
1027 **33**, 784–786 (2017).
- 1028 61. Katoh, K. & Standley, D. M. MAFFT Multiple Sequence Alignment Software Version 7:
1029 Improvements in Performance and Usability. *Molecular Biology and Evolution* **30**, 772–780
1030 (2013).
- 1031 62. Minh, B. Q. *et al.* IQ-TREE 2: New Models and Efficient Methods for Phylogenetic Inference
1032 in the Genomic Era. *Molecular Biology and Evolution* **37**, 1530–1534 (2020).
- 1033 63. Kalyaanamoorthy, S., Minh, B. Q., Wong, T. K. F., von Haeseler, A. & Jermini, L. S.
1034 ModelFinder: fast model selection for accurate phylogenetic estimates. *Nature Methods* **14**,
1035 587–589 (2017).
- 1036 64. Rambaut, A. *FigTree v1. 4.* (2012).
- 1037 65. Cresawn, S. G. *et al.* Phamerator: a bioinformatic tool for comparative bacteriophage
1038 genomics. *BMC Bioinformatics* **12**, 395 (2011).
- 1039 66. Ravantti, J., Bamford, D. & Stuart, D. I. Automatic comparison and classification of protein
1040 structures. *J Struct Biol* **183**, 47–56 (2013).
- 1041 67. Mönttinen, H. A. M., Ravantti, J. J. & Poranen, M. M. Common Structural Core of Three-
1042 Dozen Residues Reveals Intersuperfamily Relationships. *Molecular Biology and Evolution* **33**,
1043 1697–1710 (2016).
- 1044 68. Pope, W. H. & Hatfull, G. F. Adding pieces to the puzzle: New insights into bacteriophage
1045 diversity from integrated research-education programs. *Bacteriophage* **5**, e1084073 (2015).

- 1046 69. Steinegger, M. & Söding, J. MMseqs2 enables sensitive protein sequence searching for the
1047 analysis of massive data sets. *Nat Biotechnol* **35**, 1026–1028 (2017).
- 1048 70. Krupovic, M. & Koonin, E. V. Multiple origins of viral capsid proteins from cellular ancestors.
1049 *PNAS* **114**, E2401–E2410 (2017).
- 1050 71. Ravantti, J. J., Martinez-Castillo, A. & Abrescia, N. G. A. Superimposition of Viral Protein
1051 Structures: A Means to Decipher the Phylogenies of Viruses. *Viruses* **12**, 1146 (2020).
- 1052 72. Oh, B., Moyer, C. L., Hendrix, R. W. & Duda, R. L. The delta domain of the HK97 major capsid
1053 protein is essential for assembly. *Virology* **456–457**, 171–178 (2014).
- 1054 73. Mönttinen, H. A. M., Ravantti, J. J. & Poranen, M. M. Structural comparison strengthens the
1055 higher-order classification of proteases related to chymotrypsin. *PLOS ONE* **14**, e0216659
1056 (2019).
- 1057 74. Ross, P. D. *et al.* Crosslinking renders bacteriophage HK97 capsid maturation irreversible
1058 and effects an essential stabilization. *EMBO J* **24**, 1352–1363 (2005).
- 1059 75. Duda, R. L., Martincic, K., Xie, Z. & Hendrix, R. W. Bacteriophage HK97 head assembly. *FEMS*
1060 *Microbiol Rev* **17**, 41–46 (1995).
- 1061 76. Gilakjan, Z. A. & Kropinski, A. M. Cloning and Analysis of the Capsid Morphogenesis Genes
1062 of *Pseudomonas aeruginosa* Bacteriophage D3: Another Example of Protein Chain Mail? *J*
1063 *Bacteriol* **181**, 7221–7227 (1999).
- 1064 77. Fortier, L.-C., Bransi, A. & Moineau, S. Genome Sequence and Global Gene Expression of
1065 Q54, a New Phage Species Linking the 936 and c2 Phage Species of *Lactococcus lactis*. *J*
1066 *Bacteriol* **188**, 6101–6114 (2006).

- 1067 78. Hatfult, G. F. & Sarkis, G. J. DNA sequence, structure and gene expression of
1068 mycobacteriophage L5: a phage system for mycobacterial genetics. *Molecular Microbiology*
1069 **7**, 395–405 (1993).
- 1070 79. Molineux, I. J. & Panja, D. Popping the cork: mechanisms of phage genome ejection. *Nat*
1071 *Rev Microbiol* **11**, 194–204 (2013).
- 1072 80. D’Lima, N. G. & Teschke, C. M. A Molecular Staple: D-Loops in the I Domain of
1073 Bacteriophage P22 Coat Protein Make Important Intercapsomer Contacts Required for
1074 Procapsid Assembly. *Journal of Virology* (2015) doi:10.1128/JVI.01629-15.
- 1075 81. Steven, A. C., Greenstone, H. L., Booy, F. P., Black, L. W. & Ross, P. D. Conformational
1076 changes of a viral capsid protein: Thermodynamic rationale for proteolytic regulation of
1077 bacteriophage T4 capsid expansion, co-operativity, and super-stabilization by soc binding.
1078 *Journal of Molecular Biology* **228**, 870–884 (1992).
- 1079 82. Tso, D., Hendrix, R. W. & Duda, R. L. Transient contacts on the exterior of the HK97
1080 procapsid that are essential for capsid assembly. *J Mol Biol* **426**, 2112–2129 (2014).
- 1081 83. Hagan, R. M. *et al.* NMR Spectroscopic and Theoretical Analysis of a Spontaneously Formed
1082 Lys-Asp Isopeptide Bond. *Angew Chem Int Ed Engl* **49**, 8421–8425 (2010).
- 1083 84. Suhanovsky, M. M. & Teschke, C. M. Bacteriophage P22 capsid size determination: Roles for
1084 the coat protein telokin-like domain and the scaffolding protein amino-terminus. *Virology*
1085 **417**, 418–429 (2011).
- 1086 85. Earnshaw, W. C., King, J., Harrison, S. C. & Eiserling, F. A. The structural organization of DNA
1087 packaged within the heads of T4 wild-type, isometric and giant bacteriophages. *Cell* **14**,
1088 559–568 (1978).

- 1089 86. Ross, A., Ward, S. & Hyman, P. More Is Better: Selecting for Broad Host Range
1090 Bacteriophages. *Front Microbiol* **7**, 1352 (2016).
- 1091 87. Battistuzzi, F. U., Feijao, A. & Hedges, S. B. A genomic timescale of prokaryote evolution:
1092 insights into the origin of methanogenesis, phototrophy, and the colonization of land. *BMC*
1093 *Evol Biol* **4**, 44 (2004).
- 1094
1095
1096
1097
1098
1099
1100
1101
1102
1103
1104
1105
1106
1107
1108
1109
1110
1111

1112 **Supporting information**

1113 **Supporting Table 1.** Host and bacteriophage information for each bacteriophage used

1114 in this study.

Phage name	MCP pham	Cluster/Sub- cluster	Host	Genome length	Growth temp. (°C)
<i>Oxtober96</i>	15199	EA/EA1	<i>Microbacterium foliorum</i> NRRL B-24224	41798	32
<i>Bridgette</i>	15199	FA	<i>Arthrobacter globiformis</i> B- 2979	43113	32
<i>Muddy</i>	15199	AB	<i>Mycobacterium smegmatis mc²155</i>	48228	37
<i>Bobbi</i>	15199	F/F1	<i>Mycobacterium smegmatis mc²155</i>	59179	37
<i>Adephagia</i>	15199	K/K1	<i>Mycobacterium smegmatis mc²155</i>	59646	37
<i>Cain</i>	15199	K/K6	<i>Mycobacterium smegmatis mc²155</i>	60813	22
<i>Ziko</i>	15199	DP	<i>Gordonia terrae</i> 3612	68860	32
<i>Ogopogo</i>	57445	F/F1	<i>Mycobacterium smegmatis mc²155</i>	56867	37
<i>Cozz</i>	57445	CT	<i>Gordonia terrae</i> 3612	46600	32
<i>Che8</i>	4631	F/F1	<i>Mycobacterium smegmatis mc²155</i>	59471	37

1115

1116 **Supporting Table 2.** Cryo-EM collection parameters, analysis, and final resolutions.

1117

1118

Data collection	Muddy	Bridgette	Oxtober96	Ziko	Bob	Adephagia	Che8	Cozz	Ogopogo	Cain
Microscope	Titan Krios 3Gi									
High Tension / kV	300									
Pixel size / Å	1.076	0.6615	0.39915	0.4008	0.83	0.4008	0.83	0.413	0.83	0.4008
Spherical aberration / mm	2.7									
Nominal defocus / μm	1 to 2.5	1 to 3	1 to 3	1 to 3	1 to 3	1 to 2.5	1 to 3	1 to 3	1 to 3	1 to 2.5
Detector (mode)	Falcon III (Counting)	Gatan K3 (super resolution)	Gatan K3 (super resolution)	Gatan K3 (super resolution)	Falcon III (Counting)	Gatan K3 (super resolution)	Falcon III (Counting)	Gatan K3 (super resolution)	Falcon III (Counting)	Gatan K3 (super resolution)

	ing mode)			resol ution)	unti ng mod e)		mode)	resol ution)		resol ution)
Total exposure dose / eÅ ⁻²	50	23	30	26	30	24	30	24	30	25
Number of frames	48	40	32	30	32	50	32	30	32	30
Number of micrographs	1027	4303	10437	5058	191 5	5688	1201	2799	2220	4368
Number of particles in final refinement	25244	13926	13198	3595 0	189 69	51783	1497 2	4361 1	18736	3187 8
Extract box size (fourier crop box size)	800 (800)	1600 (800)	2048 (800)	2400 (750)	102 4 (686)	2400 (800)	1024 (800)	2400 (800)	1024 (800)	2400 (800)
Final pixel size used in reconstruction	1.076	1.323	1.02182	1.28 256	1.24	1.2024	1.062 4	1.239	1.0624	1.202 4

Ewald sphere correction mask diameter	710	700	650	760	750	760	750	670	750	760
Symmetry	I (I4)	I (I1)	I (I1)	I (I4)	I (I1)	I (I1)	I (I1)	I (I1)	I (I1)	I (I2)
Resolution (FSC 0.143)	2.7	4	2.2	2.6	2.5	2.4	2.5	2.6	2.7	2.9

1119

1120 **Supporting Table 3.** RMSD values of the Bobi-like (pham 15199) cryo-EM derived
 1121 major capsid protein models when compared to Bobi. Values are calculated using the
 1122 Matchmaker command in ChimeraX with default settings.

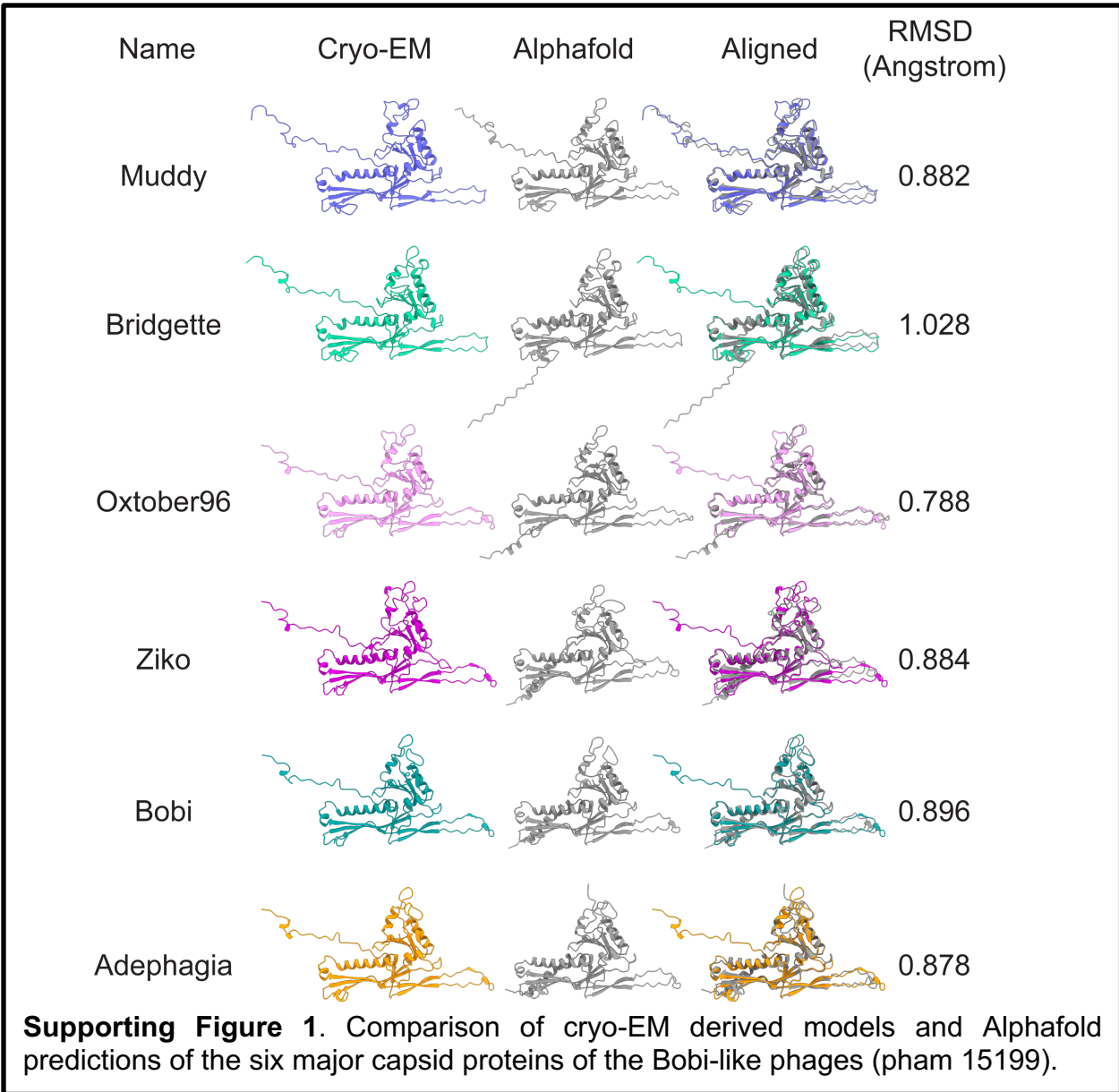
1123

Bacteriophage *RMSD (Å) compared to Bobi*

<i>Muddy</i>	1.0
<i>Bridgette</i>	1.2
<i>October96</i>	1.1
<i>Ziko</i>	1.1
<i>Adephagia</i>	0.6

1124

1125



1126

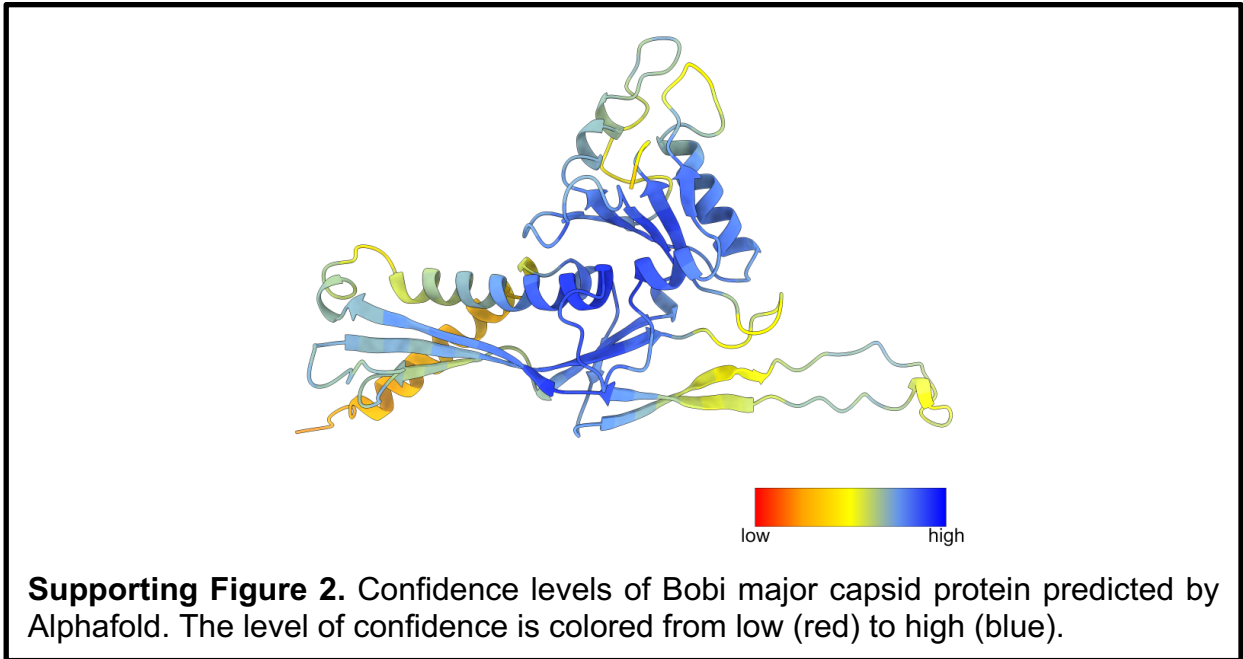
1127

1128

1129

1130

1131



1132

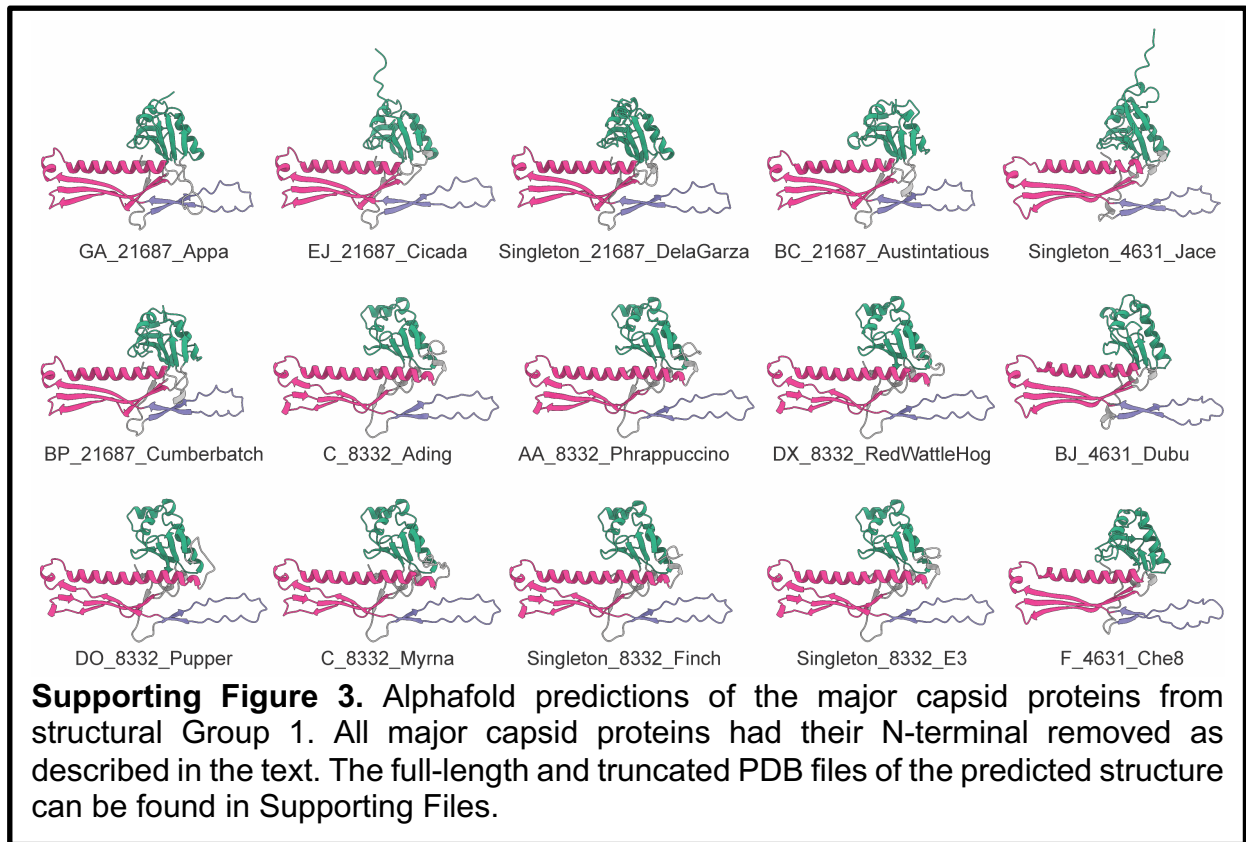
1133

1134

1135

1136

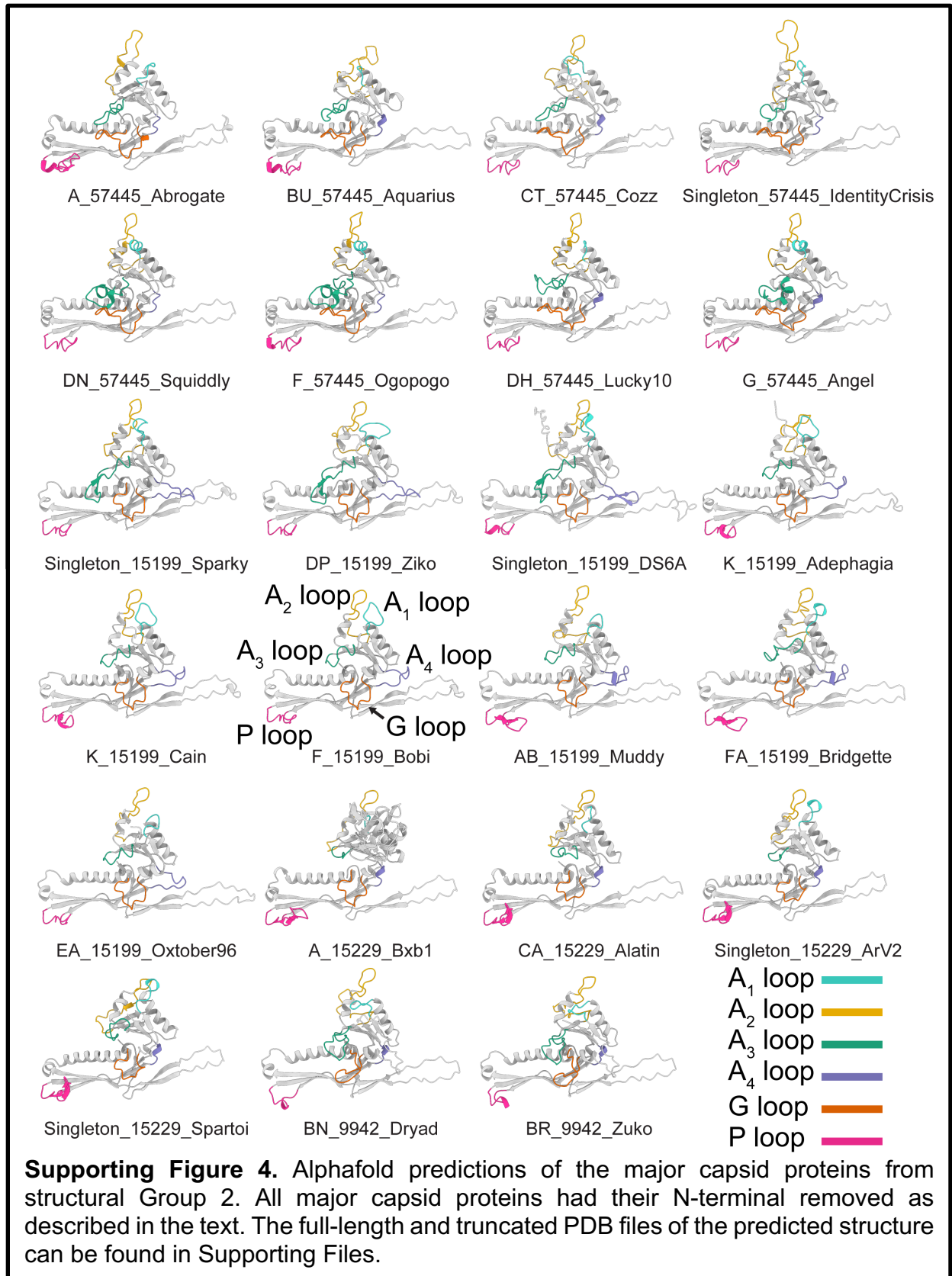
1137



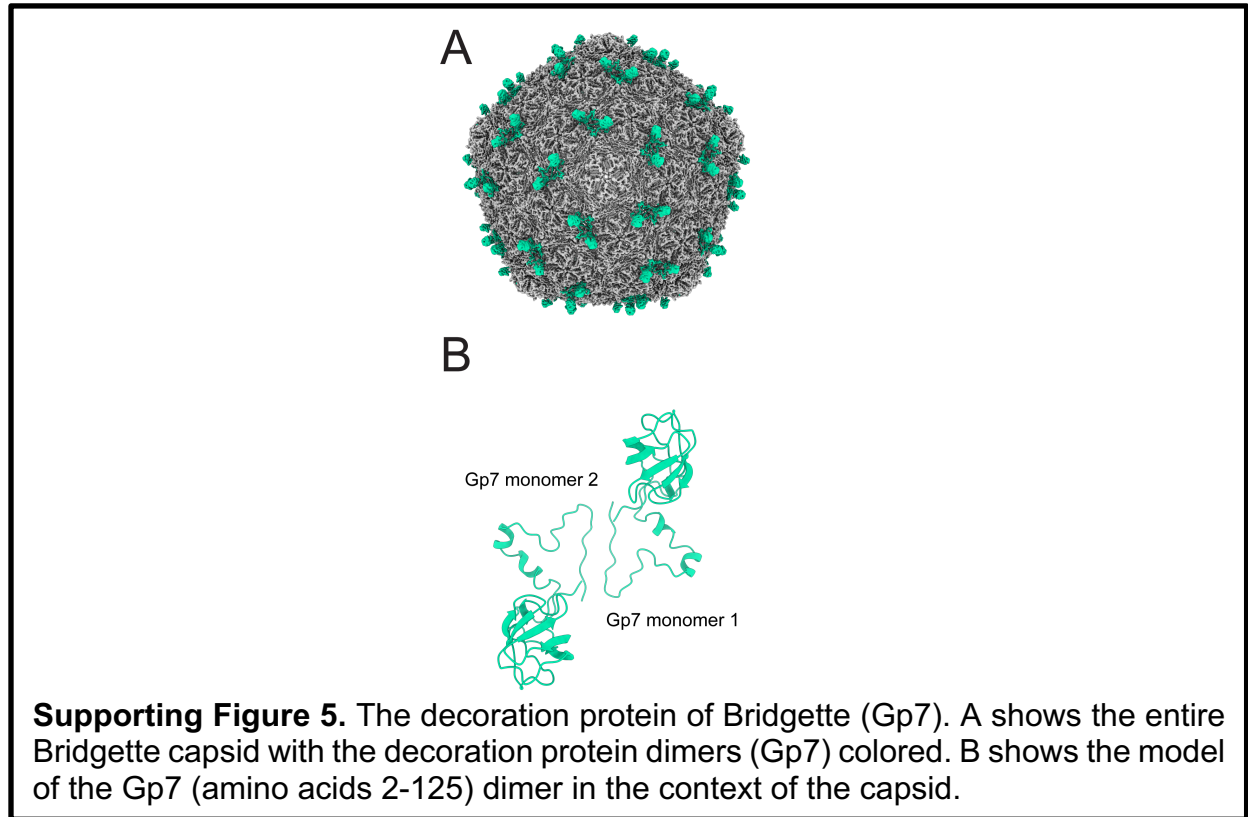
1138

1139

1140



1142



1143

1144

1145

1146

1147

1148

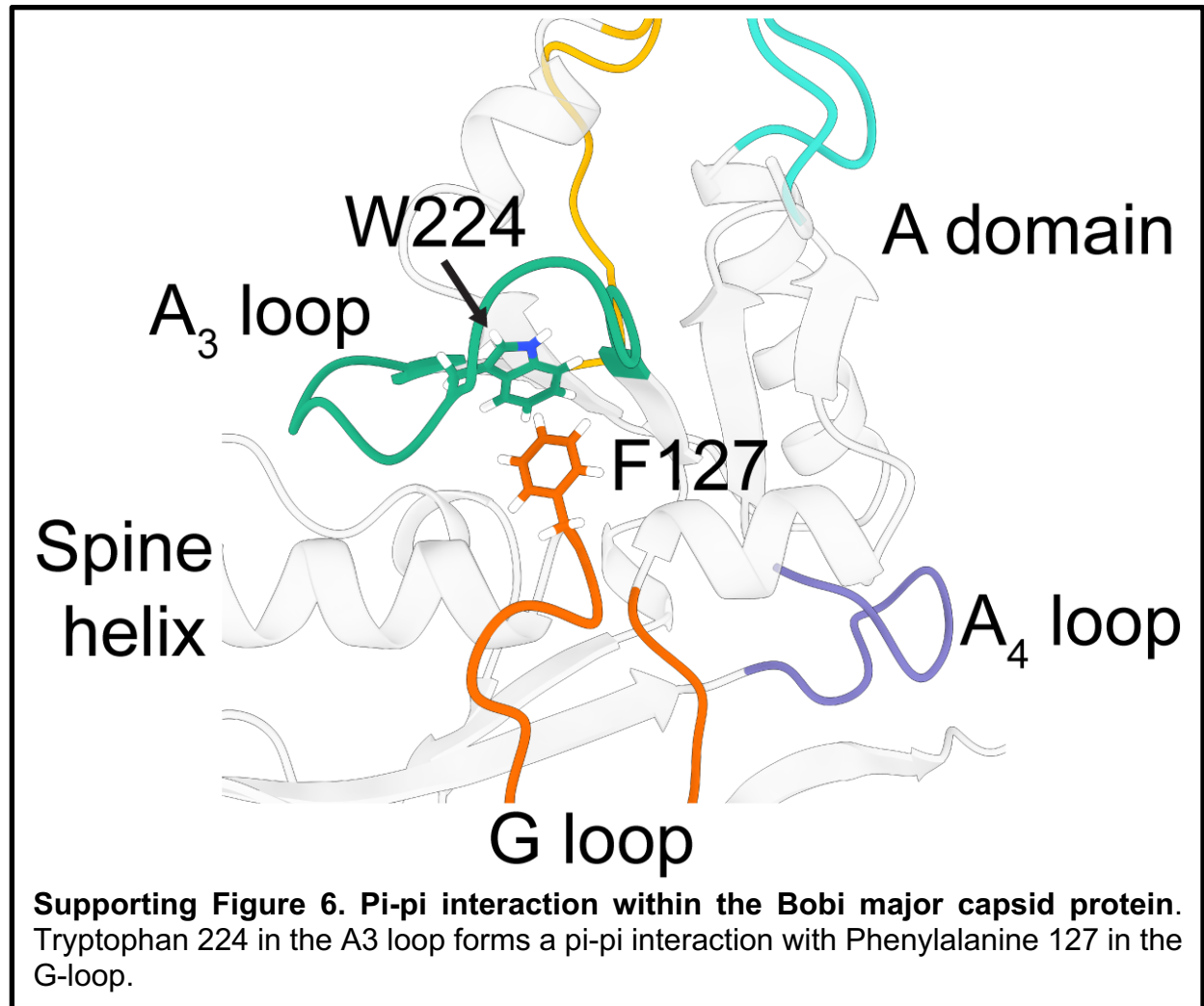
1149

1150

1151

1152

1153



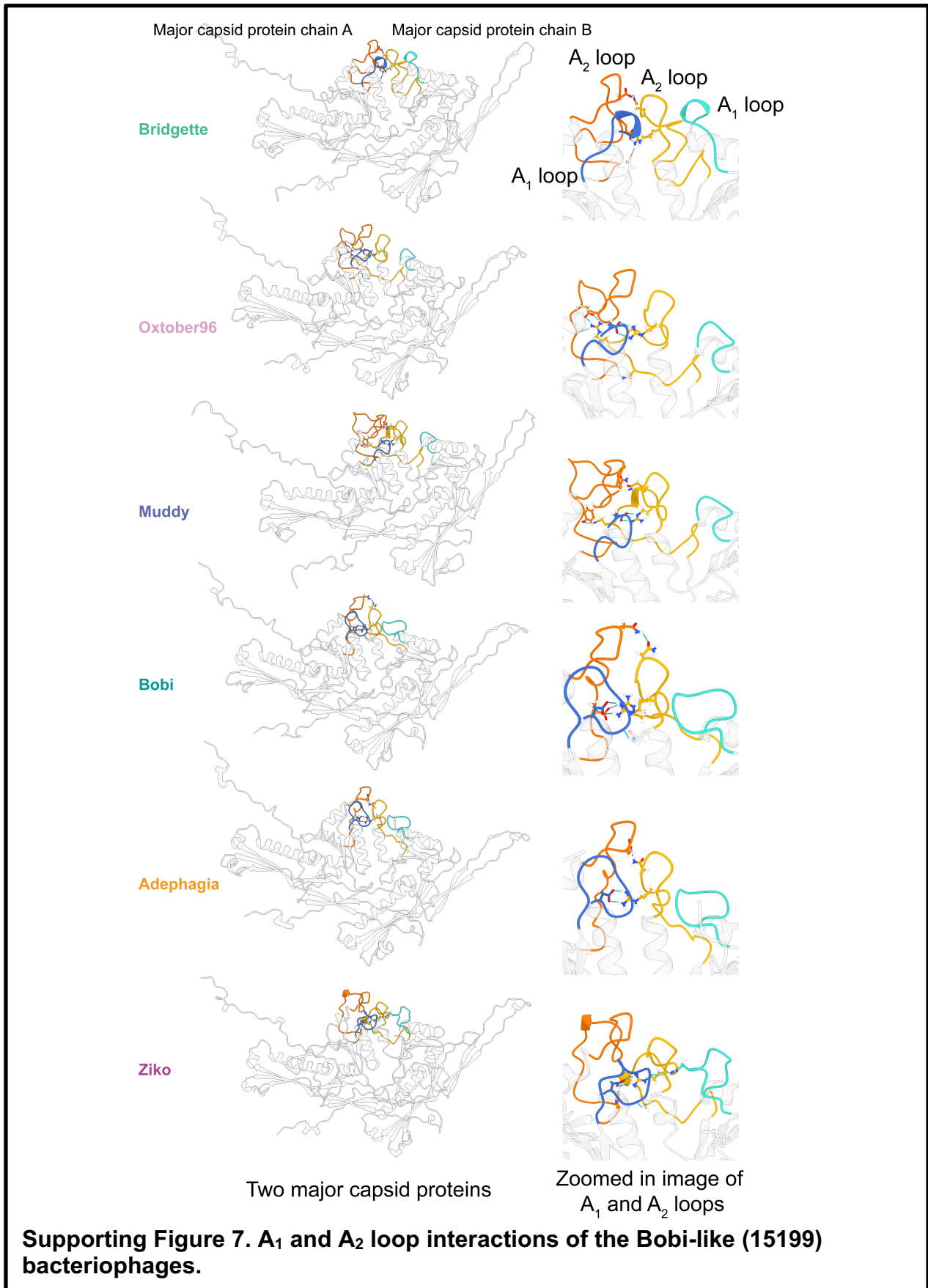
1154

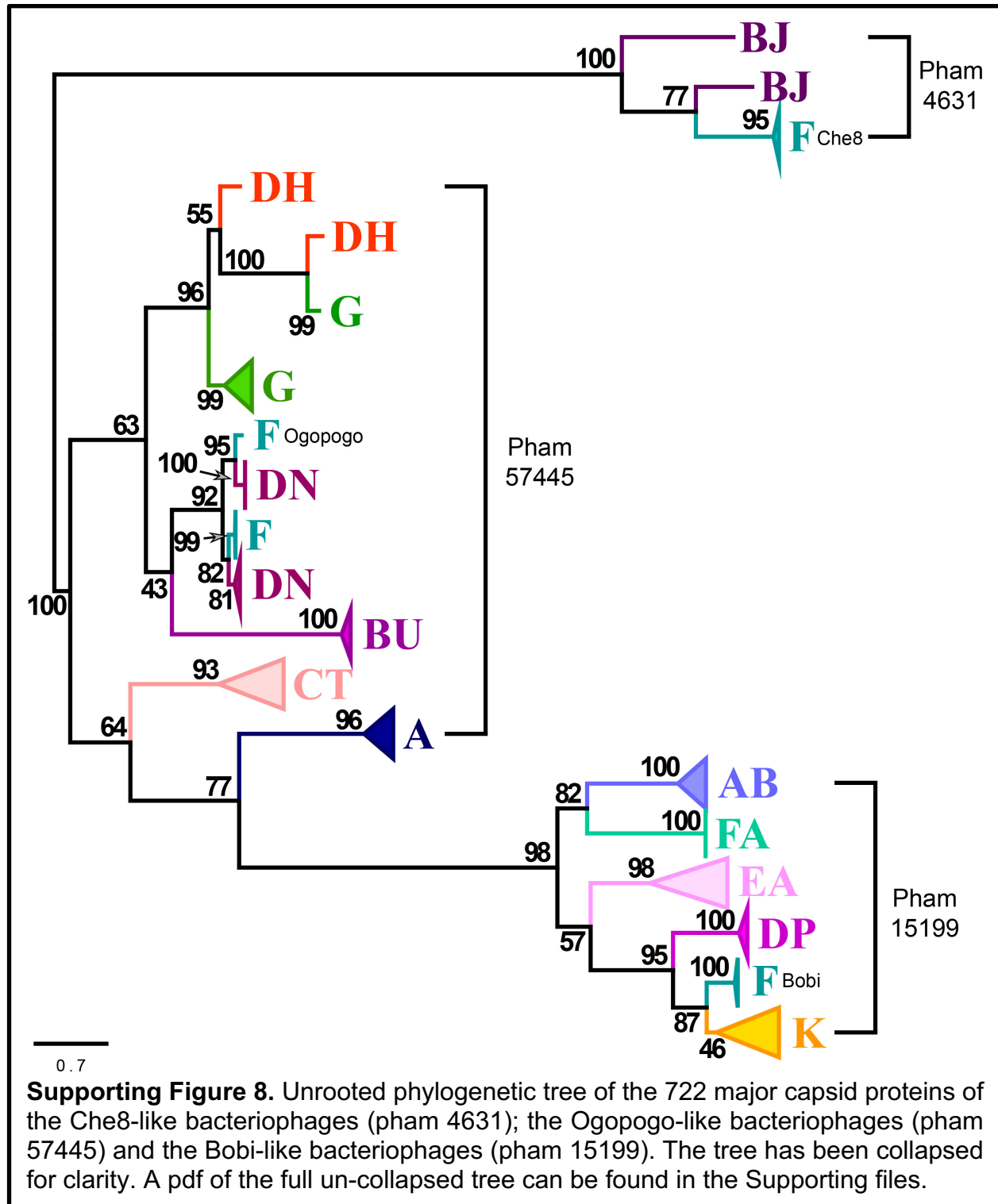
1155

1156

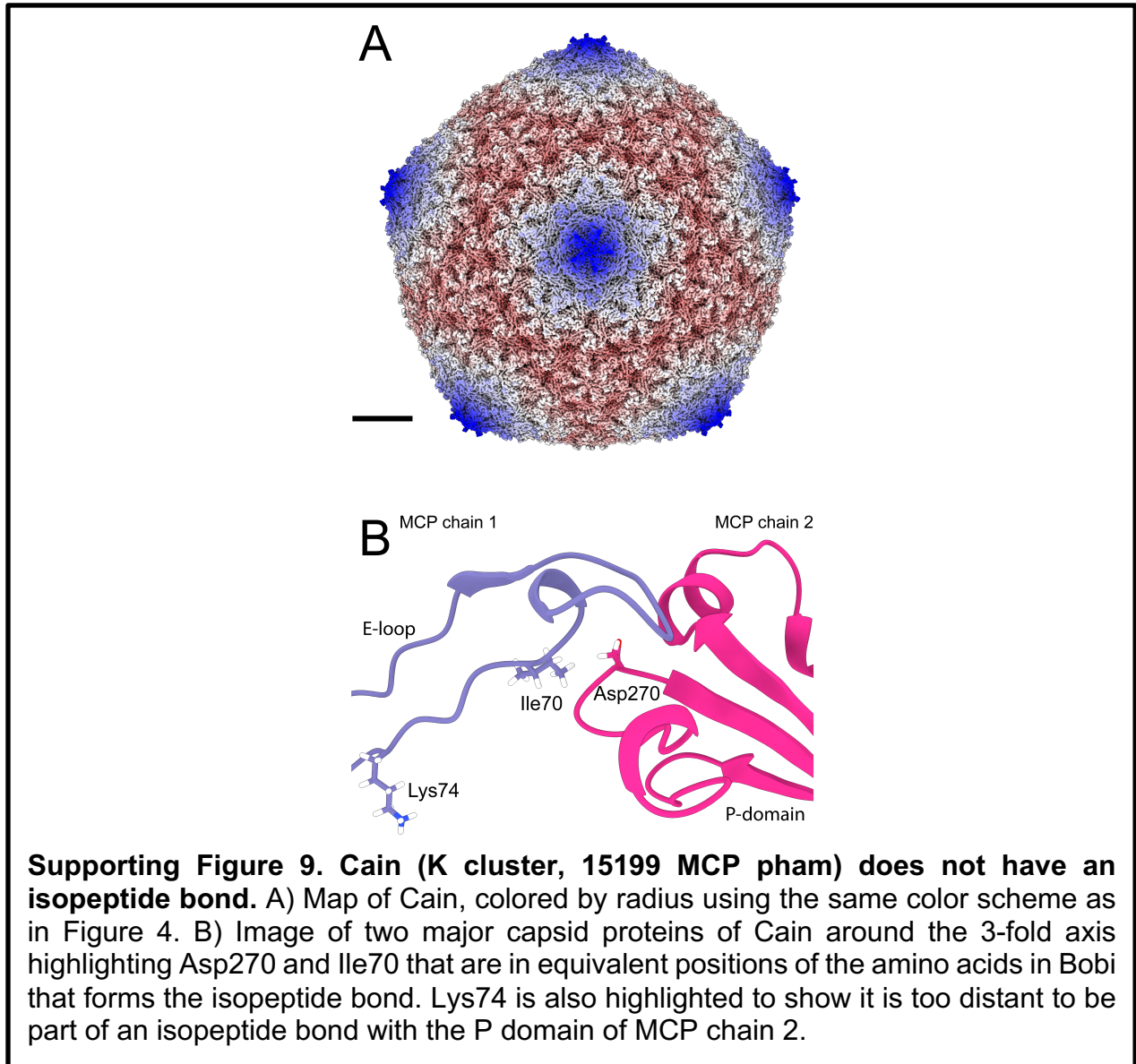
1157

1158





1160



1161

1162

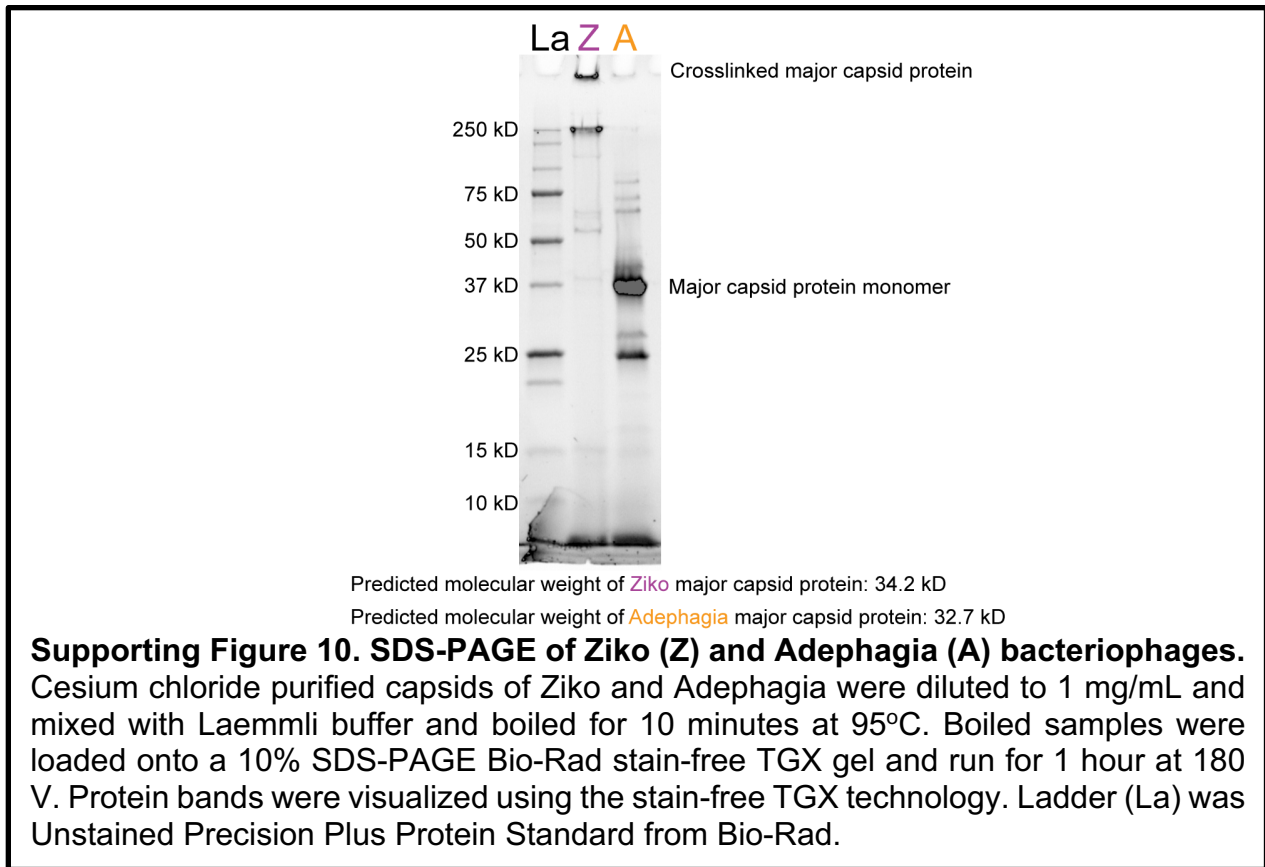
1163

1164

1165

1166

1167



1168

1169

